Journal of Environmental Health Science and Engineering (2021) 19:1851–1874
https://doi.org/10.1007/s40201-021-00740-8

RESEARCH ARTICLE

Effective Cd^{2+} removal from water using novel micro-mesoporous activated carbons obtained from tobacco: CCD approach, optimization, kinetic, and isotherm studies

Jéssica Manfrin[1] · Affonso Celso Gonçalves Junior[2] · Daniel Schwantes[3] · Juliano Zimmermann[1] · Elio Conradi Junior[1]

Received: 15 July 2020 / Accepted: 11 September 2021 / Published online: 7 October 2021

Abstract

Purpose This research aimed to develop activated carbons from tobacco by double (thermal-physical) and triple activations (thermal-chemical-physical) for high-efficiency removal of Cd^{2+}.

Methods The adsorbents were characterized by their chemical composition, point of zero charge (pH_{PZC}), SEM, FT-IR, BET, and BJH. The subsequent adsorption studies were conducted: optimal conditions (CCD on adsorbent dose *versus* pH of Cd^{2+} solution), kinetics, equilibrium, thermodynamics, and desorption studies.

Results The activated carbons have irregular and heterogeneous morphology, surface functional groups COO–, C–O, C–O–C, C=O and O–H, pH_{PZC} of 11.11 and 10.86, and enhanced SSA (especially for CT NaOH + CO_2 = 103.40 g m^{-2}). The optimal conditions for Cd^{2+} adsorption occur using 4.0 g L^{-1}, pH from 3.0 to 7.0, with most of the Cd^{2+} adsorbed in the first 10–20 min. The goodness of the fit found for pseudo-first order, pseudo-second order, intraparticle diffusion, Langmuir, Freundlich, Dubinin–Radushkevich, Sips, and Temkin suggest the occurrence of Cd^{2+} chemisorption and physisorption in mono and multilayers. The values of $\Delta G° < 0$ kJ mol^{-1} indicate that the observed phenomena are energetically favorable and spontaneous; the values of $\Delta H° < 0$ and the effective desorption rates (58.52% and 44.64%) suggest that the adsorption of Cd^{2+} is ruled mainly (but not only) by physical interactions.

Conclusion Our excellent results on Cd^{2+} removal allow us to state that tobacco use as a raw material for adsorbent development is a renewable and eco-friendly technique, allowing the production of highly effective activated carbons and providing an adequate destination for this waste.

Keywords Alternative adsorbents · Cadmium removal · CCD approach · Advanced water treatment · *Nicotiana tabacum* · Cigarettes

✉ Daniel Schwantes
daniel_schwantes@hotmail.com

Jéssica Manfrin
jessicamanfrinn@gmail.com

Affonso Celso Gonçalves Junior
affonso133@hotmail.com

Juliano Zimmermann
juliaanozimmermann@gmail.com

Elio Conradi Junior
elio.conradi@outlook.com

[1] Universidade Estadual do Oeste do Paraná (UNIOESTE), Universitária Street, 1619, Universitário, Cascavel, State of Paraná 85819-110, Brazil

[2] Pesquisador Produtividade em Pesquisa do CNPq -Nível 1C, Universidade Estadual do Oeste do Paraná (UNIOESTE), Universitária Street, 1619, Universitário, Cascavel, State of Paraná 85819-110, Brazil

[3] Departamento de Ciencias Vegetales, Facultad de Agronomía e Ing. Forestal, Pontificia Universidad Católica de Chile, Avenida Vicuña Mackenna 4860, Macul, Región Metropolitana, Santiago, Chile

Introduction

The world population reached 7.6 billion in 2017, and it is estimated to be 9.1 billion in 2050 [1]. To this increasing population, new technologies must be employed to meet the worldwide demand in various fields. More renewable and productive techniques, with lower cost than traditional ones, also that aim a better optimization of natural resources are more than needed [2].

This last statement has especial importance regarding water treatment technologies. In the last decades, industrialization, agriculture, and expanding urbanization have increased the pressure on fresh water bodies, causing high levels of pollutants, in many cases of contamination with metals [3, 4], pesticides [5–7], organic matter [8, 9], and their environmental impacts on sediments, benthic organisms, humans, i.e., the trophic chain as a whole [7, 10–13].

Among the high toxicity contaminants that have the potential for accumulation in environmental compartments and bioaccumulation in living beings, we highlight cadmium (Cd), as it is the 7th ranked substance in the "ATSDR 2019 Substance Priority List" [14]. This metal is still generated as a by-product of the mining and industrialization of Zn, Cu, and Pb [15]. For humans, one of the main risks associated with Cd is the consumption of water contaminated with this metal, either *in natura* or in the use of this water in the manufacture of beverages and food preparation [16].

Recent research has shown that humans Cd exposure may lead to the over-expression of genes responsible for the synthesis of metallothioneins (MT), genes that encode heat shock proteins (HSP), including heat shock factor 1 gene (HSF1), the master relator of the HSP pathway, and other genes involved in response to oxidative stress [17]. According to the ATSDR [18], human exposure to Cd can affect the following organ systems: Cardiovascular, gastrointestinal, neurological, urinary system (especially kidneys), reproductive and respiratory (from the nose to the lungs), damaging the organs, generally during their developing.

This toxic metal can be introduced into the environment by natural means (volcanic activities, rock weathering, and erosive process) and mainly through anthropic activities, such as industrial activities (electroplating, batteries, and electronic components), mining activities, fossil fuel combustion, municipal solid waste incineration, phosphate fertilizer manufacturing, among others [19–22]. The use of Cd became expressive only from the last century so that this metal is used in a wide variety of modern processes, such as the production of batteries, pigments, plastics, and agrochemicals [23].In addition, the production and use of this metal have increased considerably in recent decades, and, consequently, there is an increase in waste generation with this contaminant [24].

Given the problems above caused by Cd contamination, given the ecological need to improve traditional techniques to reach higher efficiencies of remediation, the development of adsorbents using low-cost alternative materials is very welcome. These materials should have high removal rates of Cd from waters, low cost of production and application, and applicable on a large scale. In this scenario, the activated carbon (AC) can be produced from different biomasses with different activation methodologies, including chemical activation (use of modifying chemical agents—NaOH, H_3PO_4, $ZnCl_2$, etc.) and physical activation (activation at high temperatures with the presence of CO_2 or water vapor). This material has high adsorptive potential, presenting excellent physical and chemical characteristics efficient in removing various contaminants [25, 26].

One material that currently does not have a proper destination and added economic value is the cigarette seized by the Federal Police in border regions of Brazil. This material, when improperly designated, can cause environmental contamination due to its high pollutant load [27]. On the other hand, its transformation into AC enables the decontamination of waters, besides providing this toxic waste a new use, promoted by science and innovation [26].

According to Ibope (Brazilian Institute of Public Opinion and Statistics), in 2018, 106.2 billion cigarettes were consumed in Brazil, of which 57.5 billion outside the legal market (Agência [28], considering that the average weight of one cigarette as 1.2 g, we estimate that 69,000 tons of tobacco were smuggled in Brazil only during 2018. The number of seizures of smuggled cigarettes has been steadily increasing year after year [27]. However, the disposal of these wastes is no longer adequate, creating environmental problems on both sides of the Brazil-Paraguay border.

Recent researches report the use of tobacco for the development of ACs and biochars: Manfrin et al. [29] developed AC from tobacco modified with $ZnCl_2$ and CO_2 for Pb^{2+} removal; Manfrin et al. [30] also performed an attempt in recycling this material producing thermal-chemical-physical changes (with H_3PO_4 and CO_2 in the tobacco for AC production; or Conradi Jr. et al. [27] who developed tobacco ACs modified with $ZnCl_2$ and NaOH. Nevertheless, all previous researches report lower metal removal rates or materials with poor characteristics. Moreover, the experimental design usually is not suitable for adequately evaluating the optimal physicochemical characteristics of the developed ACs, not using the CCD approach, or optimizing essential parameters in the adsorption [31–33, 33, 34, 34–37, 37].

Thus, this study aim (i) to enhance the development of activated carbon (AC) by using tobacco cigarettes (as a raw-matter) seized by the IRS (Internal Revenue Service) in Brazilian border regions; (ii) to produce ACs

using a double and triple activation process, aiming high-efficiency removal of Cd^{2+} from water/wastewater; (iii) to study the mechanisms of Cd^{2+} adsorption using the characterization of the new carbons (SEM, FT-IR, chemical composition, pH_{PZC}, SSA, etc.) and through adsorption studies (optimization studies, kinetics, equilibrium and thermodynamics studies).

Material and methods

Preparation and characterization of activated carbons (ACs)

The developed ACs were produced from cigarette tobacco seized in the west of Paraná State, south of Brazil, by the Internal Revenue Service (IRS). Initially, the tobacco was dried in an oven at 65 °C for a period of 24 h, crushed, and sieved for particle size standardization (0.212 to 1.40 mm), as mentioned by Conradi Jr. et al. [27]. Then, the tobacco followed two preparation methodologies: thermal-physical activations, which produced the carbon named CT *in natura* + CO_2; and thermal-physical–chemical activations, generating the carbon labeled CT NaOH + CO_2.

In the first stage (thermal activation), the pyrolysis of the tobacco was performed in a tube oven (FT 1200 1Z, with an internal dimension of 120 × 300 mm; model FE50RPN digital controller), under a continuous flow of inert gas N_2 and absence of O_2, until it reached a temperature of 750 °C. After reached 750 °C, the pyrolyzed material was physically activated under a continuous flow of CO_2 for 60 min (physical activation). Subsequently, the decanted material was washed with ultrapure water (to neutral pH) and taken to a drying oven for 4 h at 110 °C [38].

In the second stage (thermal-physical–chemical activations), the two-stage activation methodology [27, 39] was adopted, which consists of first obtaining the thermally activated material at 500 °C, under a continuous flow of inert gas N_2, for 60 min (thermal activation). Subsequently, the material was washed to neutral pH, dried, and chemically activated with 1 mol L^{-1} NaOH solution (chemical activation). The mixture containing the chemical solution and the material was set in contact for 6 h under constant stirring (200 rpm) at 45 °C. The material was separated by filtration, subjected to washing with ultrapure water, and then dried for 24 h at 65 °C. Finally, the physical activation was performed, i.e., the material was kept at 750 °C, for 60 min, under a continuous flow of CO_2. Thus, these two steps generated the two ACs from tobacco (Box 1).

After the development of the ACs, their chemical composition was determined. For this, the ACs were submitted to nitro-perchloric digestion [40], with subsequent determination of the concentrations of P, K, Ca, Mg, Cu, Zn, Mn, Fe, Cd, Pb, and Cr by FAAS [41]. The following analyses were also performed for the characterization of the obtained materials: pH of the point of zero charge (pH_{PZC}) [27], scanning electron microscopy (SEM), infrared spectroscopy (FT-IR), and porosimetry (BET and BJH).

Box 1 Description of the produced activated carbons (ACs) and their yield

ACs from tobacco	Description	Yield (Y %) $Y = \left(\frac{m_i - m_f}{m_i}\right)100$
CT *in natura* + CO_2	Thermally and physically (CO_2) AC from tobacco	43.18
CT NaOH + CO_2	Thermally, chemically (NaOH), and physically (CO_2) AC from tobacco	57.90

Adsorbent dose and the influence of solution pH (optimization study)

The optimum adsorption conditions for adsorbent dose and the pH of the Cd solution were defined by using a central composite design (CCD) [42]. Five adsorbent doses and five pH levels (adjusted by the addition of NaOH and HCl at 0.1 mol L^{-1}) were tested by using actual and coded values and four repetitions at the central point (Table S1). Adsorbent doses and pH values were combined with fixed volumes of 50 mL solution at the concentration of 10 mg L^{-1} monoelemental Cd^{2+} prepared using cadmium nitrate [$Cd(NO_3)_2$ $4H_2O$; PA ≥ 99.0% Sigma-Aldrich]. After that, the reactors were stirred in a thermostated Dubnoff system (200 rpm) for 1.5 h at 25 °C. The obtained values for the final concentration were plot in response to surface graphs.

Studies on adsorption kinetics

From the results obtained in the step above, 4.0 g of tobacco-AC was added in an Erlenmeyer flask containing 1 L of Cd^{2+} solutions [10 mg L^{-1}] at pH 5.00. For this, a reactor (Erlenmeyer) was considered for each AC (CT *in natura* + CO_2 and CT NaOH + CO_2). Then, the reactors were stirred in time intervals of 10, 20, 30, 40, 50, 60, 80, 100, 120, 140, 160, and 180 min. At each point, 15 mL aliquots were taken, filtered (on qualitative filter paper), and the residual Cd concentration was determined by FAAS [41]. In order to study the kinetics mechanism that rules the Cd adsorptive process,

the linear and non-linear models of pseudo-first order [43], pseudo-second order [44], Elovich [45], and intraparticle diffusion [46] were used.

Equilibrium studies, isotherm construction, and desorption studies

In 125 mL Erlenmeyer flasks, 4.0 g of the developed ACs were weighed and set in contact with 50 mL of Cd^{2+} solutions in the concentrations of 0, 5, 30, 60, 90, 120, 150, 180, 210, 240, 270 and 300 mg L^{-1}. The physical–chemical conditions of this procedure were: pH 5.00, system temperature 25 °C, and contact time between adsorbent/adsorbate of 45 min. After stirring, aliquots were taken to determine the Cd^{2+} residual concentration by FAAS [41]. The adsorption process was studied by the use of linear and non-linear models of Langmuir [47], Freundlich [48], Dubinin and Radushkevich [49], Sips [50], Temkin and Pyzhev [51], and Liu et al. [52].

Also, to verify the possibility of reusing the developed ACs, an evaluation using an acid elution and water (control) was performed. After the equilibrium tests (after adsorption of Cd), the recovered adsorbents were dried at 60 °C for 24 h. The obtained mass was disposed of in Erlenmeyer flasks of 125 mL and set in contact with 50 mL HCl solution (0.1 mol L^{-1}) and water (pH 7.0) for 90 min (25 °C and 200 rpm). The final concentrations of Cd (desorbed) were determined by FAAS [41].

Adsorption thermodynamics

The influence of temperature on the adsorption process was also studied. For that, 4.0 g of the ACs were weighted in 125 mL Erlenmeyer flasks and set in contact with 50 mL of Cd^{2+} solution. The physical–chemical conditions of this test were: Cd concentration of 50 mg L^{-1}, pH 5.00. 200 rpm, stirring time of 45 min, evaluated temperatures of 15, 25, 35, 45, and 55 °C. After the stirring period, aliquots were taken to determine Cd concentration by FAAS [41]. From the obtained results, the parameters of Gibbs free energy (ΔG°), enthalpy (ΔH°), and entropy (ΔS°) [53] were estimated. All mathematical models and equations employed in this research are described in Table S2 (Supplementary materials).

Results and discussion

Determination of the chemical composition of the activated carbons (ACs)

According to Li et al. [54], by applying chemical or physical activations in biomass, the characteristics of the adsorbent material are improved, such as an increase in specific surface area (SSA), better pore distribution, formation of new functional groups able to interact with pollutants, etc.

Comparing the tobacco obtained from cigarettes (raw-material) [27] (Table 1), it is possible to see that the proposed activations (thermal and physical) applied to tobacco biomass resulted in an increase in the levels of K (2.57x), Ca (2.74x), Mg (2.88x), Cu (3.10x), Zn (17.84x), Mn (1.96x), Fe (5.48x) and Pb (2.29x) in CT *in natura* + CO_2. Also, it is noticeable that the levels of Cd and Cr in cigarettes were below the LQ (limit of quantification), and the promoted method caused the partial pyrolysis of the cellulosic structures, generating CO_2, the proportion of all metals increased in the final material (including Cd, Pb, and Cr). Also, comparing the tobacco biomass to the produced CT NaOH + CO_2, the same process is evident, with an increase ("accumulation" of metals due to loss of volatile biomass during the pyrolysis) of the concentrations of the metals K (0.27x), Ca (1.60x), Mg (2.65x), Cu (2.30x), Zn (21.26x), Mn (2.24x), Fe (4.59x) and Pb (3.37x). In this case, it is also possible to observe that Cd and Pb concentrations are below LQ in the cigarette biomass; nevertheless, the pyrolysis and the partial loss of the cellulosic structures caused an increase

Table 1 Chemical composition of CT *in natura* + CO_2 and CT NaOH + CO_2 and rate of increase concerning the natural tobacco metal concentration (biosorbent)

Adsorbents	P	K	Ca	Mg	Cu	Zn	Mn	Fe	Cd	Pb	Cr
	g Kg^{-1}				mg kg^{-1}						
Tobacco Conradi Jr et al. [27]	5.92	44.80	26.10	5.88	10.00	19.00	283.00	175.67	< LQ	26.67	< LQ
CT *in natura* + CO_2	< LQ	115.15	71.40	16.95	31.00	339.00	555.00	963.00	20.00	61.00	25.00
	–	2.57x	2.74x	2.88x	3.10x	17.84x	1.96x	5.48x	–	2.29x	–
CT NaOH + CO_2	< LQ	12.05	41.80	15.60	23.00	404.00	633.00	806.00	4.00	90.00	36.00
	–	0.27x	1.60x	2.65x	2.30x	21.26x	2.24x	4.59x	–	3.37x	–

LQ (limits of quantification): K = 0.01, Ca = 0.005, Mg = 0.005, Cu = 0.005, Fe = 0.01, Mn = 0.01, Zn = 0.005, Cd = 0.005, Pb = 0.01 and Cr = 0.01 (mg kg^{-1})

in the proportion of these metals in the final product. Other volatile elements, such as P, with a boiling point of 277 °C, are entirely lost during the thermal activations and production of ACs (Table 1).

The incomplete pyrolysis applied to tobacco ultimately removed a significant portion of the volatile solids in the biomass since the activation from activating chemical solutions or the insertion of the material at high temperatures can extract or modify part of the elements that constitute the initial material [55, 56].

In addition, washing off the material after pyrolysis to neutral pH may have influenced the variation of the metal concentration by diluting some of them after the pyrolysis. Schwantes et al. [57] also observed changes in the chemical composition of cassava materials after chemical activation (by using solutions of 0.1 mol L^{-1} of H_2SO_4, NaOH, and H_2O_2) and washing.

Similar results were found by Conradi Jr. et al. [27] using thermal activation on tobacco biomass, followed by chemical activation using NaOH or $ZnCl_2$; these authors also evidence an increase in most metals concentration in the resulting ACs, also with lower accumulation when using NaOH as an activator.

According to Overend et al. [58], chemicals such as $ZnCl_2$ can cause an effect of influence pyrolysis as a catalyst, i.e., the decomposition starts at a lower temperature. However, when basic catalysts are used (NaOH, such in this research), the beta-bonding exhibits lower stability. According to the authors above, in the presence of NaOH, cellulose starts to decompose earlier than amylose, and the wide range of possible reactions in the pyrolysis of carbohydrate may be bracketed between two extreme possibilities:

(1) Dehydration $C_6H_{12}O_6 \rightarrow 6C + 6H_2O$ (40% residue)
(2) Rearrangement $C_6H_{12}O_6 \rightarrow 3CH_3COOH$ (or $3CH_4 + CO_2$)

The pH related to the point of zero charge (pH_{PZC})

The pH_{PZC} obtained for CT *in natura* + CO_2 is 11.11 and 10.86 for CT NaOH + CO_2 (Fig. 1). According to Pezoti et al. [59], the pH_{PZC} corresponds to the point of zero charge on the surface of the adsorbent, i.e., when the pH_{PZC} > pH of the solution, the adsorbent surface will prefer anion adsorption, otherwise when pH_{PZC} < pH of the solution, the adsorbent surface will prefer cation adsorption.

However, it is essential to mention that the pH_{PZC} allows predicting the adsorptive preference regarding physical interactions. As adsorption is a very complex process, which can be ruled by chemical affinity or physical interactions, the pH_{PZC} can only provide a partial idea of one type of interaction that can occur [60]. The results found for pH_{PZC} are directly influenced by the performed chemical activation and precursor material characteristics. In this sense, Conradi Jr. et al. [27] observed similar values in the ACs from tobacco modified by $ZnCl_2$ and NaOH, with pH_{PZC} values of 5.40 (for biosorbent—tobacco), 7.47 for the AC modified with $ZnCl_2$, and 12.84 for the AC modified with NaOH.

Hassan, Abdel-Mohsen, and Fouda [61] state that physical activations performed with CO_2 allow a high amount of volatile materials to be released and that due to the numerous reactions that occur during the process, the pH of the material may become more alkaline, consequently, influencing the pH_{PZC} of the ACs, just as observed in Fig. 1.

Cansado et al. [62] developed AC from a mixture of synthetic polymers, and according to their findings, by using different ratios of KOH and K_2CO_3, the pH_{PZC} varied from 7.19 to 10.8. The increase in the alkalinity can be attributed to the formation of carbonates during pyrolysis, as observed in FT-IR analysis.

The theory behind the pH_{PZC} determination technique assumes that H^+ protons and OH^- hydroxyl groups are potential determinant ions. In an aqueous solution, the adsorbent surface may adsorb OH^- or H^+ ions. Thus, surface clusters of each active site may dissociate or associate protons from the solution, depending on the adsorbent properties and the pH of the solution. Consequently, the surface of the active sites becomes positively charged when associated with protons coming from the solution under acidic conditions or negatively charged when protons are lost to the solution under alkaline conditions [63].

Under the experimental conditions of pH (3.0 to 7.0 in adsorption studies), positive surface charges predominate, favoring the adsorption of anions. However, for higher pH values, such as alkaline effluents (11–13), negative charges in the surface of the ACs will predominate, which can favor the adsorption of cations [27], such as Cd^{2+} and other metals.

Scanning electron microscopy (SEM)

The micrographs obtained by SEM (Fig. 2) evidence the surface morphology of the developed ACs. For both materials, it is possible to observe irregular and heterogeneous structures with subtle spongy aspects (in some parts, indicated by the red arrow). A similar observation was made by Conradi Jr. et al. [27] by developing ACs from tobacco using $ZnCl_2$ and NaOH as chemical modifiers. Also, Li et al. [54] observed the formation of an irregular network structure in the ACs produced from cigarette butt waste (chemically activated with K_2CO_3).

Different results were obtained by Zhang et al. [64] by developing ACs from cigarette filters (chemically activated with KOH). The authors above state that the ACs exhibited smooth wired morphology, with the promoted pyrolysis

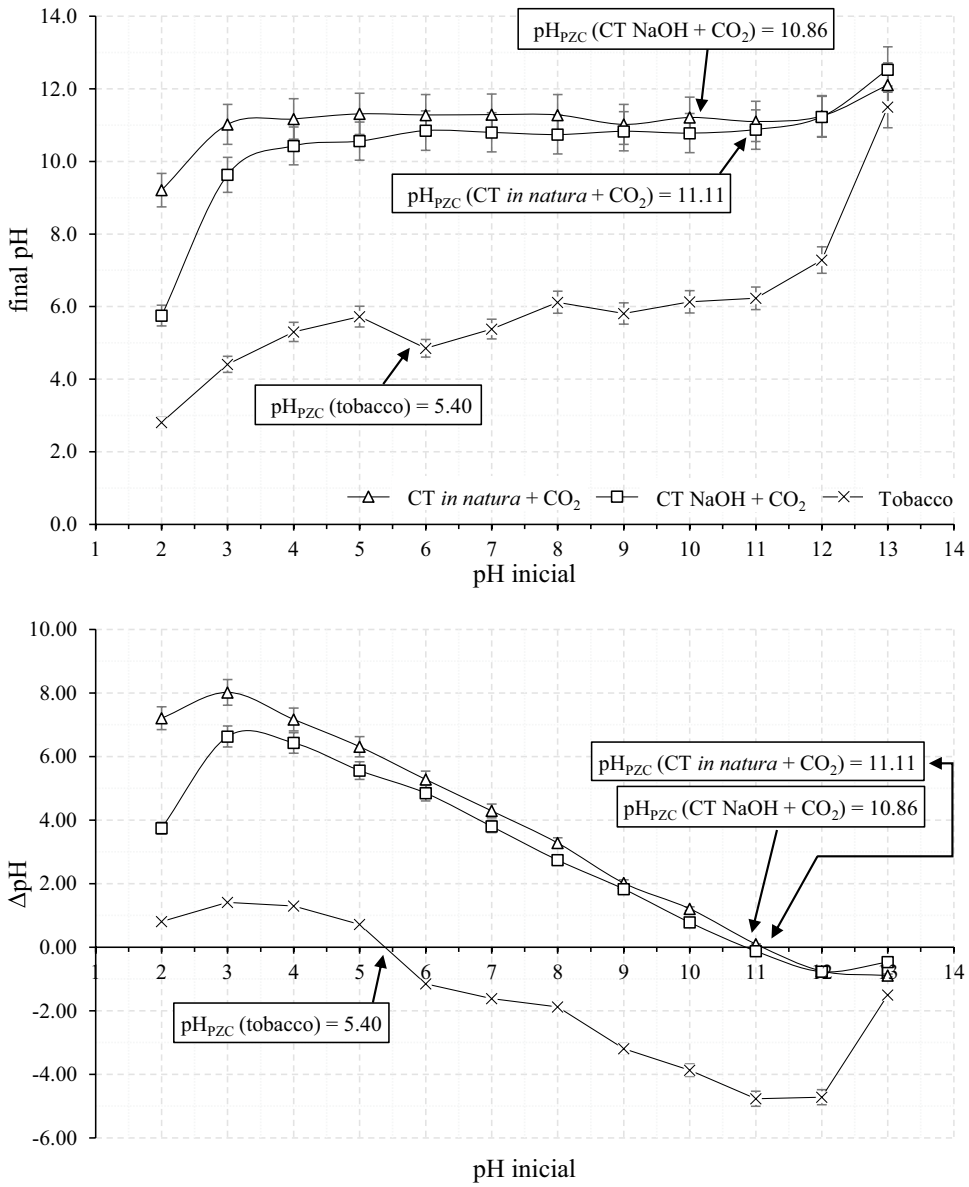

Fig. 1 pH_{PZC} of the biosorbent from tobacco and CT *in natura* + CO_2 and CT NaOH + CO_2

changing cigarette filters into irregular particulate AC with a grain size of several micrometers. These discrepant results only show that the morphology of the final adsorbent depends a lot on the raw material of origin. In Zhang's studies, it is a fibrous raw material (cigarette filters), whereas, in the present study, ACs were developed 100% from tobacco without the filters (usually made with cotton).

For both materials (CT *in natura* + CO_2 and CT NaOH + CO_2), it is possible to see their similitude by observing the cellulosic structure of the tobacco cells (Fig. 2—a and d, red arrows). However, looking at closer approximations (Fig. 2f and c), it is possible to evidence some differences between the ACs, as CT NaOH + CO_2 is irregular and heterogeneous, but not as irregular as CT *in natura* + CO_2. Thus, the chemical treatment tends to decrease the irregularity of surface structure.

Similar results were found by Schwantes et al. [55] by applying NaOH as a chemical treatment in pinus barks biosorbents. According to the authors above, the use of NaOH, a strong base with high solubility, can cause alkaline degradation of polysaccharides in the surface structure of the adsorbent materials, which may have caused these subtle differences.

Infrared spectra of adsorbents (FT-IR)

The vibrational stretches observed near 3430–3480 cm^{-1}, for both (CT *in natura* + CO_2 and CT NaOH + CO_2), suggest the presence of O–H stretch [65], inferring the presence of

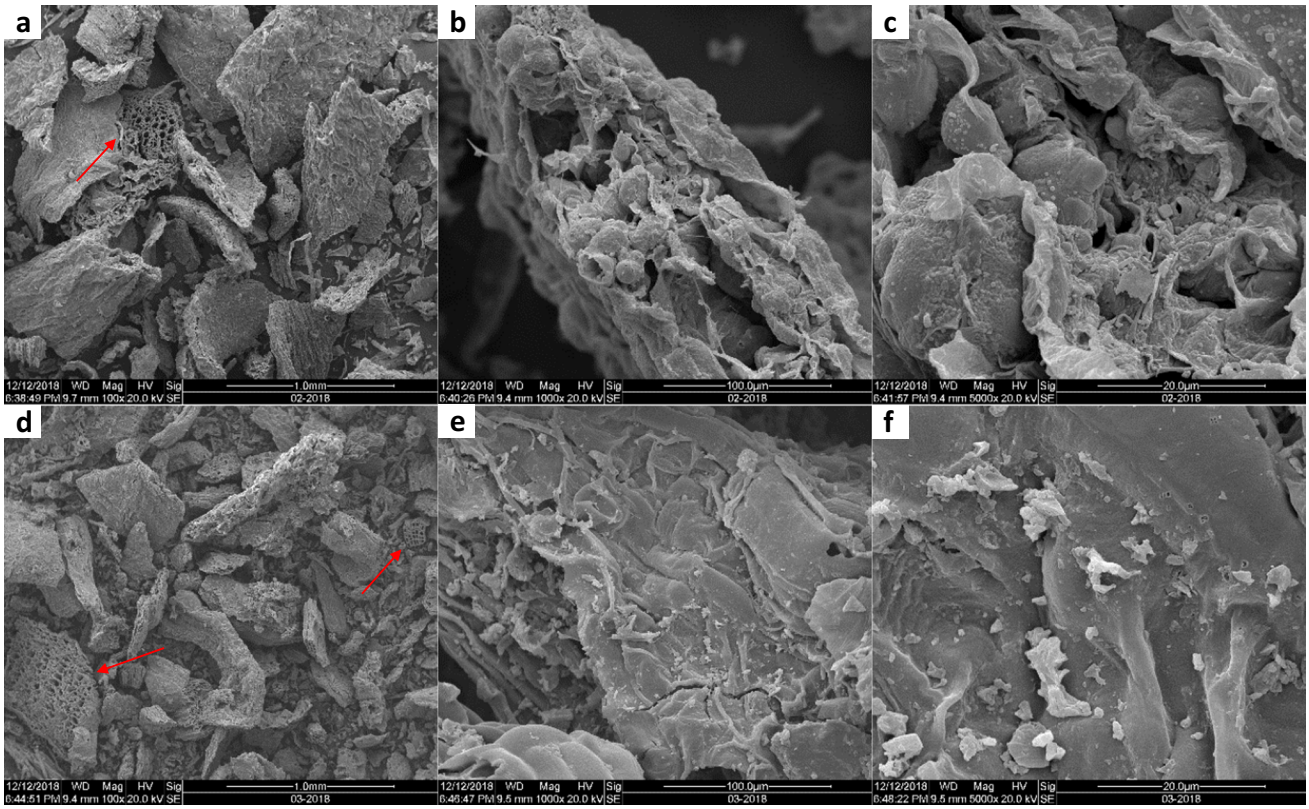

Fig. 2 Micrographs (SEM) of CT *in natura* + CO_2 [100x (**a**), 1000x (**b**) and 5000x (**c**) times] and CT NaOH + CO_2 [100x (**d**), 1000x (**e**) and 5000x (**f**) times]

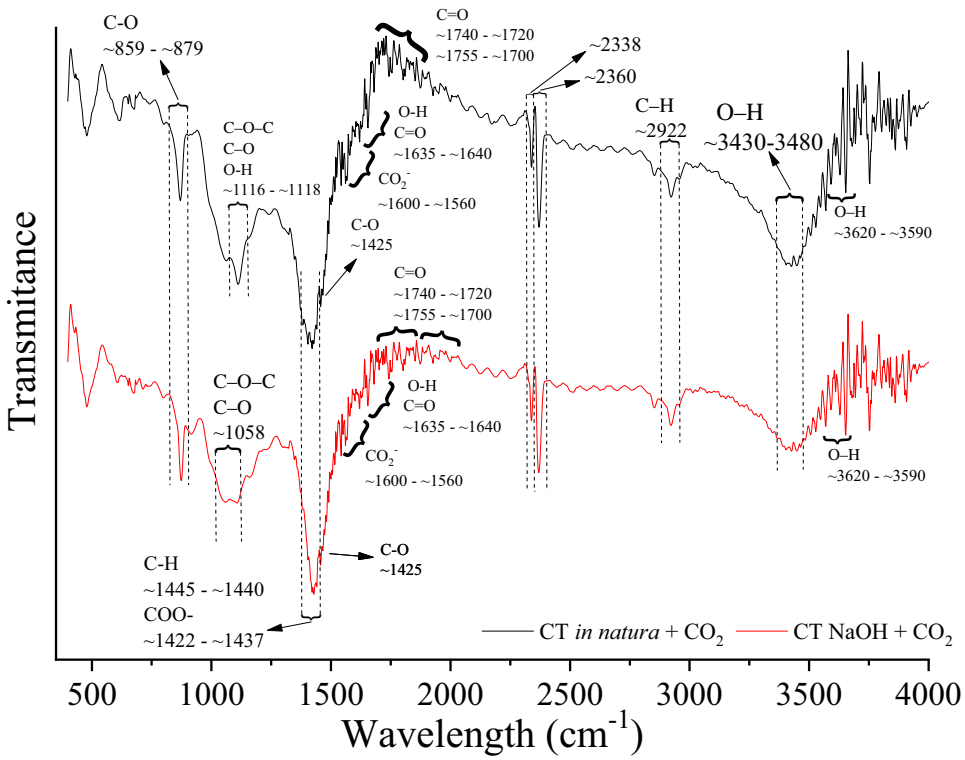

Fig. 3 Infrared spectrum from 4000 to 400 cm^{-1} for CT *in natura* + CO_2 and CT NaOH + CO_2

water [66] and O–H bonds in cellulose structure (Fig. 3). According to Silverstein et al. [67], peaks near 1635 cm^{-1} can also indicate O–H bend for absorbed water.

According to Schulz and Baranska [68], the positions and intensities of the OH stretching vibration bands vary for the different polymorphic forms of cellulose. According to the authors above mentioned, one of the forms can be a strong band near 3430 cm^{-1} and 3380 cm^{-1} [69], as observed for both ACs. These bands all exhibit dichroism, and intensity differences are also observed for different forms near 1430 cm^{-1} and 1110 cm^{-1} [69].

Phenols have an absorption band at 3620–3590 cm^{-1} due to the O–H stretching vibration [67],some sharp peaks are found in that region for both ACs, suggesting their presence.

Amino acids are amine derivatives of carboxylic acids and contain several amino and carboxylic acid groups [69]. Amino acids, polypeptides, and proteins are related compounds, and their infrared spectra reflect this to a certain extent [65]. Peaks in the range of 1250–900 cm^{-1} can indicate C–O–C and C–O form polysaccharides [67]. The peaks around 1515–1505 cm^{-1} suggest the aromatic skeletal of lignin [65].

The peaks at 1425 cm^{-1} indicate COO^- stretch; 1265–1240 cm^{-1} indicates C–O; 1640 cm^{-1} indicates C=O for carboxylates; all indicate carboxylic acids in the ACs [68]. The peaks found at 1740–1720 cm^{-1} can indicate C=O for aldehyde, ketone, carboxylic acids, and esters [69].

Free amino acids also have carboxylate ion CO_2^- stretching vibrations, a strong band occurring in the region 1600–1560 cm^{-1} can indicate its presence [69]. Dicarboxylic acids have a strong band due to the C=O stretching vibration of the carboxyl group at 1755–1700 cm^{-1} [69].

The infrared spectra of inorganic carbonates consist of robust broadband at 1495–1410 cm^{-1} [70]. Also, according to Smidt and Meissl [65], peaks at 2520 cm^{-1} and 1425 cm^{-1} (C–O stretch) can also suggest the presence of carbonate. The peaks ~ 2922 cm^{-1} in both ACs indicate C–H stretching [66]. The peaks found between 2100 to 1500 cm^{-1} can suggest C=C stretching from Alkenyl [66].

Vibrational stretches between 1445 and 1440 nm^{-1} were identified that suggest C–H bands, deducing the presence of lipids, polysaccharides, and proteins [68]. Moreover, it can be observed in the adsorbent vibrational strains related to the presence of amines and hydroxyls (1118 and 1058 nm^{-1}) present in lignin (possibly due to the precursor material—tobacco) [67]. The vibrational stretches observed at 879 nm^{-1} and 859 nm^{-1} deduce the presence of C–O, also suggesting the presence of carbonates in the adsorbents [65].

The chemical modification promoted by the oxidation (by the use of NaOH) of the carbon surface introduces more hydrophilic surface with an increase of oxygen functional groups, which can be an excellent method for the development of high-efficiency adsorbents, such as the produced by Kim et al. [39] by the modification with NaOH. These authors also found the groups' carboxyl acid, O–H stretching, C–H, $C–H_2$, and $C–H_3$ bonds, which could be favorable for the adsorption of metal ions, such as Cd^{2+}.

N_2 adsorption/desorption analysis (BET and BJH)

A considerable increase in the surface area (SSA) of the AC produced by thermal, physical, and chemical activation (CT NaOH + CO_2) in comparison with the material activated thermally and physically (CT *in natura* + CO_2) is observed in Table 2. Thus, it is possible to consider that the thermal-chemical-physical activation is the main responsible for this considerable increase in SSA [71] for the tobacco carbons.

When comparing the results observed for CT NaOH + CO_2 with a gold-standard from the literature

Table 2 Porosimetry characterization of adsorbents CT *in natura* + CO_2 and CT NaOH + CO_2 and a comparison with other adsorbents from literature

Material/Authors	Parameters			
	Specific superficial area $_{(BET)}$ ($m^2\ g^{-1}$)		Average pore volume ($cm^3\ g^{-1}$)	Average pore diameter (nm)
CT *in natura* + CO_2 (this research)	2.39	0.0090		1.54
CT NaOH + CO_2 (this research)	103.40	0.0285		1.67
AC – NaOH wheat bran [72]	71 to 2278	0.052 to 1.790		1.84 to 3.08
AC fiber [39]	1421.7 to 1588.6	0.4929 to 0.5982		0.7 to 0.8 nm
AC—KOH/NaOH [73]	51 to 1038	0.05 to 0.80		3 to 34
Ulva lactuca AC [74]	345.40	0.320		1.85
AC Tobacco [75]	121.28	0.1514		4.99
AC Tobacco—NaOH [27]	76.61	0.0525		0.060
AC Tobacco—ZnCl2 [27]	479.40	0.06012		1.67
Biosorbent from tobacco [27]	0.27	0.0008		2.18

[AC fibers modified with NaOH cited by Kim et al. [39]], it is observed that the mentioned adsorbent exhibits 1588 $m^2\ g^{-1}$, that is, 15 × greater SSA than the evidenced by CT NaOH + CO_2. However, it should be noted that the product developed by Kim et al. [39] is from pure AC fibers, a product of the highest purity and quality. In contrast, CT NaOH + CO_2 is produced from tobacco residues (apprehensions of cigarettes by the Brazilian Federal Court), i.e., zero cost and high availability.

Other authors demonstrate that by using other vegetal raw materials, such as wheat bran [72], banana peels [73], or seaweed [74], AC with enhanced SSA, pore-volume, and pore diameter were generated (Table 2). However, when comparing our findings with other ACs developed from tobacco wastes [27, 75], it is possible to observe that the CT NaOH + CO_2 have a significant improvement in SSA (103.4 $m^2\ g^{-1}$), pore volume (0.028 $cm^3\ g^{-1}$) and pore diameter (1.67 nm). Moreover, in this comparison, it is essential to state that most authors use pure or ideal raw materials to develop ACs, whereas, in our research, we used a residue, i.e., with zero cost and high availability.

In addition, the treatment (thermal-physical–chemical activation) proposed in the development of CT NaOH + CO_2 evidence an increase of 382 × in SSA and 35 × in pore volume regarding the biosorbent produced from tobacco wastes by Conradi Jr. et al. [27].

There is a proximity between the produced tobacco carbons in terms of pore diameter (Table 2). Results show that the tobacco ACs exhibit a predominantly microporous structure, with a pore diameter < 2.00 nm [76], and this is one of the main characteristics of excellent adsorbents [73].

As shown in Fig. 4, the N_2 isotherm obtained for CT *in natura* + CO_2 is characterized as type V, with a typical behavior of a mesoporous solid, proceeding through monolayer and multilayer hysteresis followed by capillary condensation [77, 78]. This classification also states that the observed behavior for N_2 adsorption/desorption occurs due to the mesoporous structure CT *in natura* + CO_2 and its weak interaction with the N_2 in the surface [79]. In these isotherms, it is possible the occurrence of multilayer of adsorption. Therefore, the isotherm inflection point (as indicated in Fig. 4 by the black arrows) corresponds to the formation of the first adsorbed layer covering the entire surface of the material. On the other hand, for CT NaOH + CO_2, a type I isotherm is observed, i.e., typical for microporous solids, limited by monolayer formation [78].

Adsorbent dose and the effect of the pH (optimization study)

The factor "Adsorbent Dose" (L and Q) presented statistical difference at the level of 1% (Table 3) for both ACs (CT *in natura* + CO_2 and CT NaOH + CO_2). The evaluated pH range (3.0 to 7.0) does not significantly influence Cd^{2+} removal, and there is no significant interaction between the factor "Adsorbent Dose" and the factor "pH" in the evaluated conditions.

Table 3 Analysis of Variance (ANOVA) for the influence of adsorbent doses and the pH solution on Cd^{2+} removal for CT *in natura* + CO_2 and CT NaOH + CO_2

Sources of variation (SV)	Degrees of freedom (GL)	Mean squares	
		CT *in natura* + CO_2	CT NaOH + CO_2
Dose (L)	1	18,766.97**	12,183.50**
Dose (Q)	1	3,903.13**	3,921.22*
pH (L)	1	0.00 ^{ns}	220.96 ^{ns}
pH (Q)	1	22.69 ^{ns}	2.52 ^{ns}
Dose x pH	1	0.01 ^{ns}	613.95 ^{ns}
Error	6	107.95	554.78
Total	11		

L linear; *Q* Quadratic

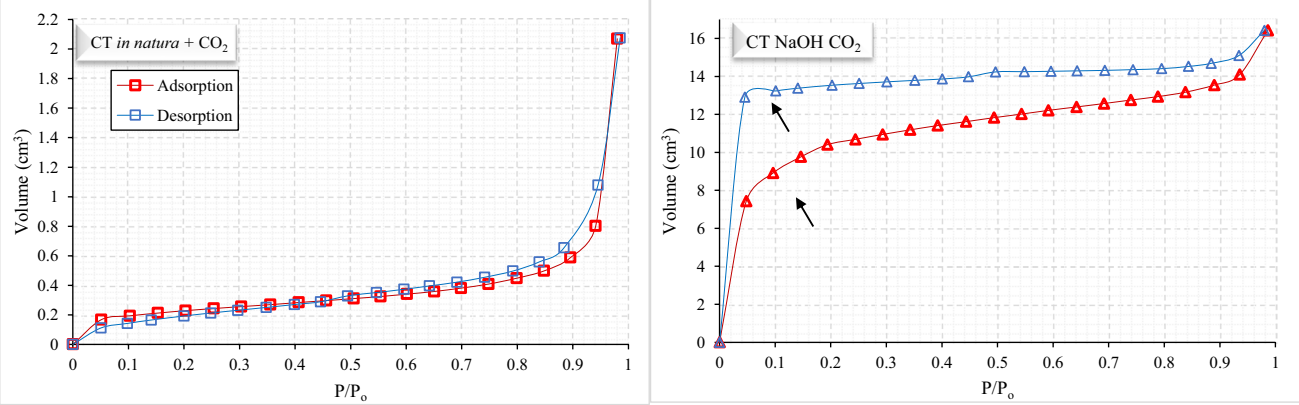

Fig. 4 Adsorption and desorption BET isotherms of CT *in natura* + CO_2 and CT NaOH + CO_2

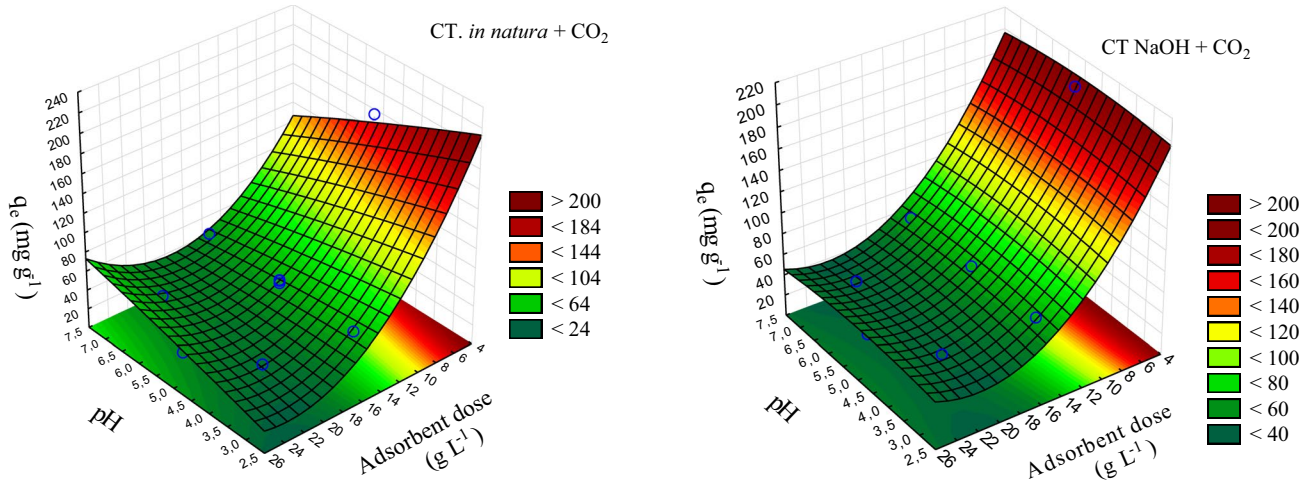

Equations		
CT *in natura* + CO_2	$q_{e\,(calc)} = 348.6166 - 19.2792x - 0.3151x^2 - 26.5756y + 0.4945y^2 + 1.2464xy$	Adj. $R^2 = 0.702$
CT NaOH + CO_2	$q_{e\,(calc)} = 256.1204 + 9.5350x - 0.9457x^2 - 21.6168y + 0.4934y^2 - 0.0041xy$	Adj. $R^2 = 0.949$

Fig. 5 Response surfaces for Cd^{2+} removal as a function of adsorbent dose (Masses: 200 to 1400 mg or 4 g L^{-1} to 28 g L^{-1}) and pH of Cd solution (3.0 to 7.0). Experimental conditions: 1.5 h of stirring, 200 rpm, and 25 °C. Details of CCD are exhibited in Table S1

The decrease in adsorptive capacity due to the increase of adsorbent dose (Fig. 5) may be related to the formation of agglomerates in the material, reducing the surface area and, consequently, the adsorptive capacity, as already observed by Schwantes et al. [56] by evaluating grape stem adsorbents for Cd^{2+} removal from water. In this preliminary study (optimization study), it is possible to evidence that CT *in natura* + CO_2 removed 100% of Cd^{2+} when using the lower adsorbent doses regardless of the evaluated pH (optimal conditions of adsorption). In comparison, CT NaOH + CO_2 removed 82% of Cd^{2+} when used the lowest proportion of the adsorbent (for both materials, the best result was predicted using doses < 8 g L^{-1}).

Similar results were obtained by Schwantes et al. [56] by evaluating the Cd^{2+} uptake capacity by using grape stem adsorbents and Gonçalves Jr. et al. [80] by using the açaí berry (amazon fruit) biosorbent in the removal of Cd^{2+}, Pb^{2+}, and Cr^{3+} from water. For the authors above, the best adsorption rates were found using adsorbent doses around 4–8 g L^{-1}.

Adsorption kinetics and comparison between linear and non-linear models

The studies of the kinetics of adsorption are essential to elucidate the dynamics of the reactions that occur during the adsorptive process [81]. After 10 min, 94% of Cd^{2+} is removed by CT *in natura* + CO_2. In comparison, only 82% is removed for CT NaOH + CO_2 during the same period of time$_2$, with a gradual increase in the adsorption rate, until 160 min, where more than 97% of Cd^{2+} is effectively adsorbed (Fig. 6-A).

This show that the adsorption of Cd^{2+} by the developed ACs is a fast process, especially for CT *in natura* + CO_2, while for CT NaOH + CO_2, it is observed a fast Cd^{2+} uptake (from 0 to 10 min) firstly, with subsequent slowly uptake of Cd^{2+} (from 10 to 180 min). This result may corroborate with the observed behavior in N_2 adsorption/desorption isotherms (Fig. 4), as CT NaOH + CO_2 has a higher pore volume (3 × higher than CT *in natura* + CO_2) and higher SSA (43 × higher than CT *in natura* + CO_2). These results may indicate a redistribution of the Cd^{2+} on the adsorbent surface; since the most energetic adsorption sites are already occupied, less energetic sites can compete to remove Cd^{2+} from the solution in a slower and more gradual process.

Based on Pholosi et al. [82] findings, we can state that the mechanism of Cd^{2+} adsorption onto the tobacco AC particles can consists of the following basic steps, (i) diffusion of Cd^{2+} from the solution to the liquid film on the adsorbent surface, (ii) diffusion of Cd^{2+} across the liquid film on the adsorbent surface, (iii) Cd^{2+} adsorption on the active sites on the surface, the strength of the bonding depending on whether the process is physical or chemical and (iv) diffusion of metal ions through pores of different sizes in the adsorbent particles (intraparticle diffusion).

The values observed for pseudo-first order (Table 4) indicate physical interactions between Cd^{2+} and the CT *in natura* + CO_2 surface, where, in this particular case, are observed adj-R^2 values of 0.98 and 0.99 (for linear and non-linear model respectively), with low values of RRS

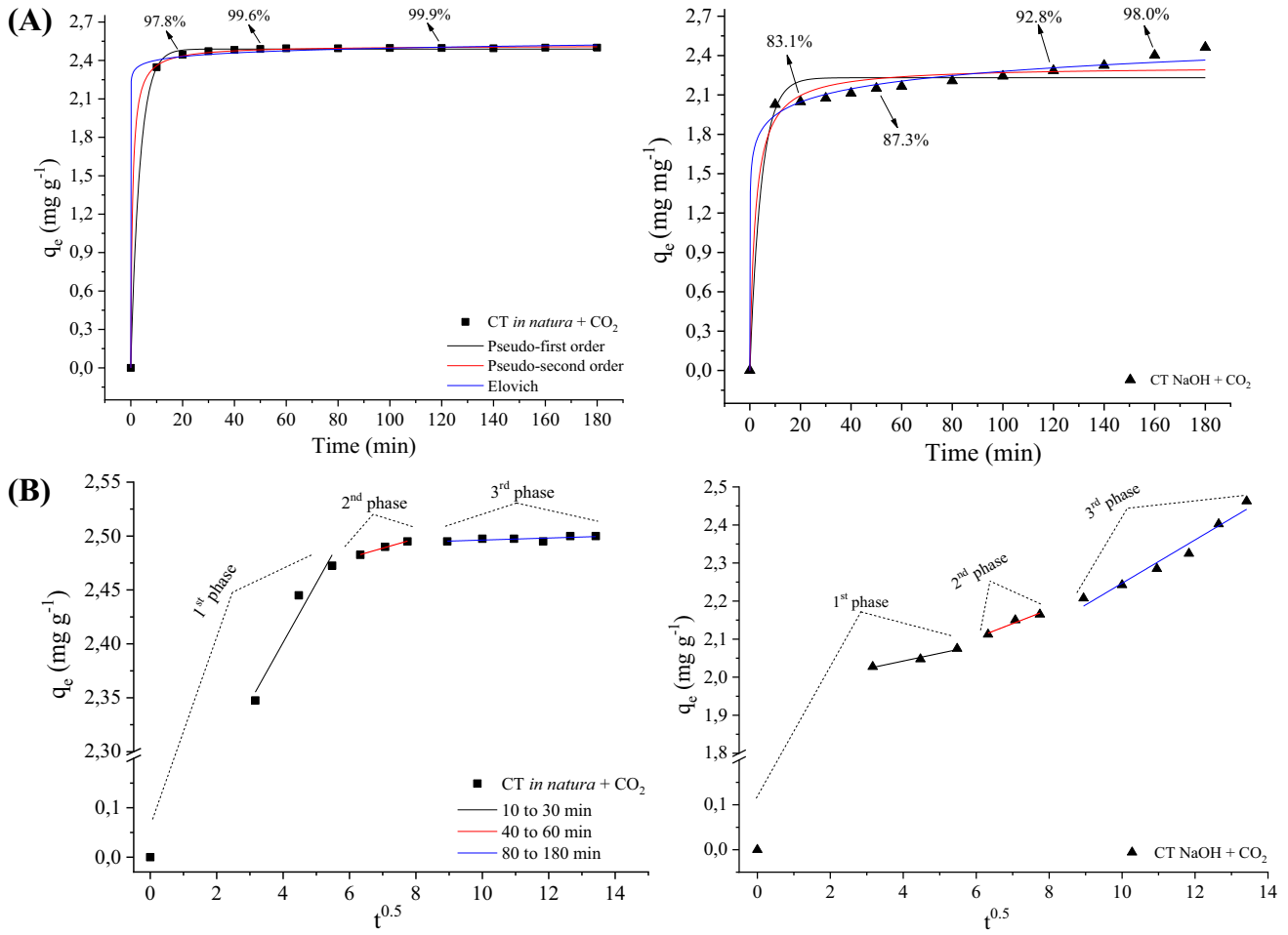

Fig. 6 **A** The contact time effect as described by the non-linear kinetics models of pseudo-fist order, pseudo-second order, and Elovich, and **B** as described by the linear model of Weber and Morris for CT *in natura* + CO_2 and CT NaOH + CO_2 in Cd^{2+} adsorption systems

(Residual Sum of Squares) and with the similarity between the values obtained for q_e (calc.) = 2.489 (non-linear) and q_e (exp.) = 2.476 mg g^{-1}. Also, even for CT NaOH + CO_2, with lower adjust values (adj-R^2 = 0.96), the prediction made by the non-linear model of pseudo-first order is quite precise, with q_e (calc.) = 2.231 and q_e (exp.) = 2.209 mg g^{-1}. These results may suggest that physical interactions have an essential role in the Cd^{2+} adsorption for both materials. It is also observed that the linear parameters of pseudo-first order failed in the prediction of q_e (exp.) values.

Excellent adjusts are observed for pseudo-second order (linear and non-linear), with values of adj-$R^2 > 0.98$ for CT *in natura* + CO_2 and CT NaOH + CO_2. Moreover, in those cases, the lower values of RRS obtained for the models' parameters and the good predictions of q_e (calc.), i.e., the proximity between q_e (calc.) and q_e (exp.), suggests that the adsorption is also ruled by the chemical affinity between Cd^{2+} and AC surfaces. According to Schwantes et al. [55], the pseudo-second order model describes well the chemical adsorption processes involving electron donation or exchange between adsorbate and adsorbent as covalent and ion exchange forces. For the author above, pinus barks chemically modified with H_2O_2, H_2SO_4, and NaOH 1 mol L^{-1} showed a high adjustment correlation for the pseudo-second order model, also suggesting the occurrence of chemisorption.The values of k_1 and k_2 obtained by the nonlinear models of pseudo-first order and pseudo-second order for CT *in natura* + CO_2 (k_1 = 0.283 min^{-1}; k_2 = 0.596 g mg^{-1} min^{-1}) and CT NaOH + CO_2 (k_1 = 0.221 min^{-1}; k_2 = 0.203 g mg^{-1} min^{-1}) were higher than the found by Müller et al. [83], when evaluating the adsorption kinetics of methylene blue in sawdust from *Pinus elliottii* (pinus) and *Drepanostachyum falcatum* (bamboo) (values of k_1 from 0.017 to 0.029 min^{-1}; values of k_2 from 0.005 to 0.0088 g mg^{-1} min^{-1}). Both of these constants (k_1 and k_2) are adsorption rate constant, demonstrating that the adsorption of Cd^{2+} by tobacco ACs is a fast process compared to the adsorption of methylene blue by sawdust of pinus or bamboo.

Table 4 Linear and non-linear kinetics parameters for Cd^{2+} removal by CT *in natura* + CO_2 and CT NaOH + CO_2

Parameters/Adsorbents	CT *in natura* + CO_2		CT NaOH + CO_2		CT *in natura* + CO_2		CT NaOH + CO_2	
	RRS		RRS		RRS		RRS	
Pseudo-first order (linear) $\log(qe - q_t) = \log qe - \left(\frac{k1}{2.303}\right)t$					Pseudo-first order (non-linear) $q_t = q_{eq}(1 - e^{-k_1 t})$			
k_1 (min^{-1})	0.065	0.002	0.009	0.009	0.283	0.010	0.221	0.053
q_e (cal.) (mg g^{-1})	0.233	0.069	0.429	0.009	2.489	0.004	2.231	0.038
Adj-R^2	0.980		0.990		0.999		0.961	
Pseudo-second order (linear) $\frac{t}{qt} = \frac{1}{k2qe2} + \frac{1}{Qe}t$					Pseudo-second order (non-linear) $q_{eq} = \frac{k_2 q_e^2 t}{1 + k_2 q_e t}$			
k_2 (g mg^{-1} min^{-1})	1.163	0.137	0.081	0.669	0.596	0.004	0.203	0.060
q_e (cal.) (mg g^{-1})	2.504	3.25 e^{-4}	2.442	0.007	2.516	0.003	2.318	0.039
Adj-R^2	0.999		0.999		0.999		0.979	
Elovich (linear) $Qeq = A + B\ Int$					Elovich (non-linear) $q_e = \frac{1}{b}\ln(1 + abt)$			
A (mg g^{-1} h^{-1})	2.446	0.007	0.011	0.086	1.61 e^{23}	1.9e^2	9201.695	15,076.120
B (g mg^{-1})	1.375	0.002	0.198	0.019	24.531	4.861	6.868	0.795
Adj-R^2	0.877		0.918		0.998		0.994	
Intraparticle diffusion (Weber-Morris) $q_e = k_{id} t^{1/2} + C_i$								
Adsorbent	CT *in natura* + CO_2							
Parameters	Line A (10 to 30 min)			Line B (40 to 60 min)			Line C (80 to 180 min)	
k_{id} (g mg^{-1} $min^{-1/2}$)	0.055 (RRS 0.013)			0.008 (RRS 7.59 e^{-4})			9.48 e^{-4} (RRS 4.73 e^{-4})	
C_i (mg g^{-1})	2.181 (RRS 0.059)			2.427 (RRS 0.005)			2.487 (RRS 0.005)	
Adj-R^2	0.889			0.985			0.377	
Adsorbent	CT NaOH + CO_2							
Parameters	Line A (10 to 30 min)			Line B (40 to 60 min)			Line C (80 to 180 min)	
k_{id} (g mg^{-1} $min^{-1/2}$)	0.020 (RRS 0.003)			0.037 (RRS 0.008)			0.057 (RRS 0.006)	
C_i (mg g^{-1})	1.961 (RRS 0.015)			1.880 (RRS 0.057)			1.677 (RRS 0.066)	
Adj-R^2	0.945			0.910			0.960	
Average D_i (cm^2 s^{-1})	CT *in natura* + CO_2 = 3.3e^{-10} (RRS 1.7e^{-10})						CT NaOH + CO_2 = 3.5e^{-10} (RRS 1.8e^{-10})	
Average q_e (exp.) (mg g^{-1})	CT *in natura* + CO_2 = 2.476 (RRS 0.044)						CT NaOH + CO_2 = 2.209 (RRS 0.139)	

k_1: rate constant of pseudo-first order; q_e: the amount of adsorbate retained per gram of adsorbent at equilibrium; k_2: rate constant of pseudo-second order; A: constant indicating the initial chemisorption rate; B: number of suitable sites for adsorption, related to the extent of surface coverage and the activation energy of the chemo reaction; k_{id} (g mg^{-1} $min^{-1/2}$): intraparticle diffusion rate constant; C_i (mg g^{-1}): reflects the boundary layer effect or surface adsorption. D_i (cm^2 s^{-1}): diffusion coefficient of intraparticle diffusion. RRS: residual sum of squares. Adj-R^2: adjusted coefficient of determination

In experimental conditions of this research, the best adjustments (for kinetics models) were found for the non-linear models, with excellent adj-R^2 for pseudo-second order and good adj-R^2 for pseudo-first order. A similar conclusion was found by Moussout et al. [81] by comparing both models (pseudo-first order and pseudo-second order), aiming for a better interpretation of batch adsorption experiments for Cd^{2+} and other contaminants.

The Elovich model (linear and non-linear), on the other hand, did not present good adjusts for the ACs or showed

overestimation, with low adj-R^2 and high RRS values, i.e., these results are not suitable for the elucidation of the observed adsorption process. Elovich equation is often used to describe chemisorption predominantly on highly heterogeneous sorbents. It is based on the assumption that the sorption sites increase exponentially with sorption, implying multilayer sorption [84].

Figure 6B shows that the plot q_e versus $t^{0.5}$ do not pass through the origin, which according to Pholosi et al. [82], the intraparticle diffusion is not the only rate-limiting step for Cd^{2+} uptake. For the tobacco-ACs, the Weber-Morris model presented satisfactory adjustments (adj-R^2 and RRS) in some cases, thus evidencing the limiting steps of the Cd^{2+} adsorption process, i.e., deducing the movement of Cd^{2+} particles to inside the pores of the adsorbent (Fig. 6B).

As shown in Fig. 6B and Table 4, both materials demonstrate that at least part of the adsorption phenomenon can be explained by intraparticle transfer, given that the material has marked porosity. Figure 6B (left) shows that the intraparticle diffusion is not linear throughout the process, suggesting that the diffusion mechanism is not dominant. In the case of CT *in natura* + CO_2, data can be easily represented by three linear phases equilibrium (1st phase: boundary layer effect and external mass transfer effect, followed by the 2nd phase: diffusion of molecules to internal sites and, the 3rd phase: with the reduction in the intraparticle diffusion) [85].

For CT NaOH + CO_2, as it is a more porous material than CT *in natura* + CO_2 (Table 2), the possibility of diffusing Cd^{2+} into the pores (CT NaOH + $CO_{2\ \text{pore volume}}$ > CT *in natura* + $CO_{2\ \text{pore volume}}$), or even redistributing the ions on the surface is greater (CT NaOH + $CO_{2\ \text{SSA}}$ > CT *in natura* + $CO_{2\ \text{SSA}}$). Here also separated into three phases (Fig. 6B right), it is observed that in the first phase we have removal from 82 to 84% of Cd^{2+}, which increases in the second phase from 85 to 88%, and that finally in the third phase it evolves from 89 to 100%.

Moreover, for both materials, the values of D_i are within the range of 10^{-5} to 10^{-13} cm^2 s^{-1}, which according to Pholosi et al. [82], indicates that the intraparticle diffusion plays an essential role in the rate-limiting step of Cd^{2+} adsorption, especially for chemisorption systems.

Adsorption equilibrium studies and comparison between linear and non-linear forms of isotherms

The linear and non-linear isotherms of Langmuir, Freundlich, Dubinin–Radushkevich, Sips, Temkin, and Liu are exhibited in Figs. 7, 8, and 9. The linear and non-linear parameters of Langmuir exhibited similar adjustments (adj-R^2 ranging from 0.96 to 0.97), with also certain similarities among the results. Moreover, the linear form of the model exhibited lower RRS for Langmuir parameters. The q_{max} values observed are 76.62 mg g^{-1} (linear) and 94.27 mg g^{-1} (nonlinear) for CT *in natura* + CO_2, and 82.51 mg g^{-1} (linear) and 75.64 mg g^{-1} (nonlinear) for CT NaOH + CO_2, indicating a high capacity of Cd^{2+} adsorption in monolayers by tobacco ACs.

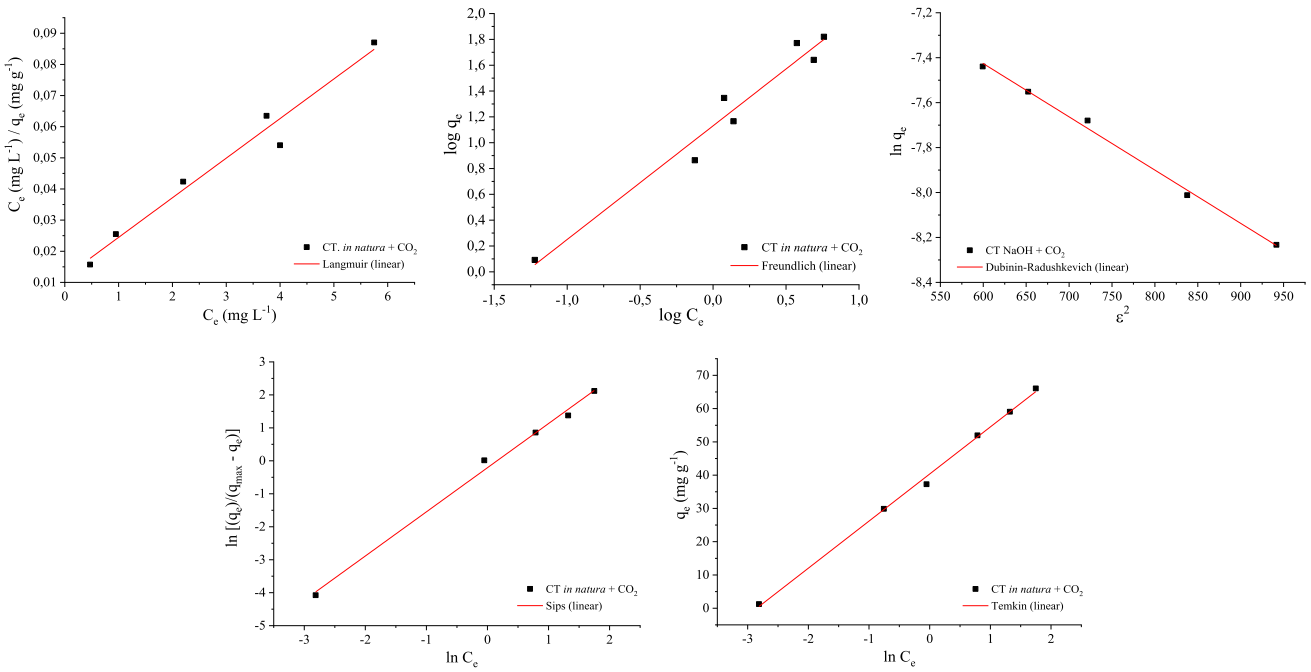

Fig. 7 Langmuir, Freundlich, Dubinin–Radushkevich, Sips, and Temkin linear isotherms (CT *in natura* + CO_2 removing Cd^{2+})

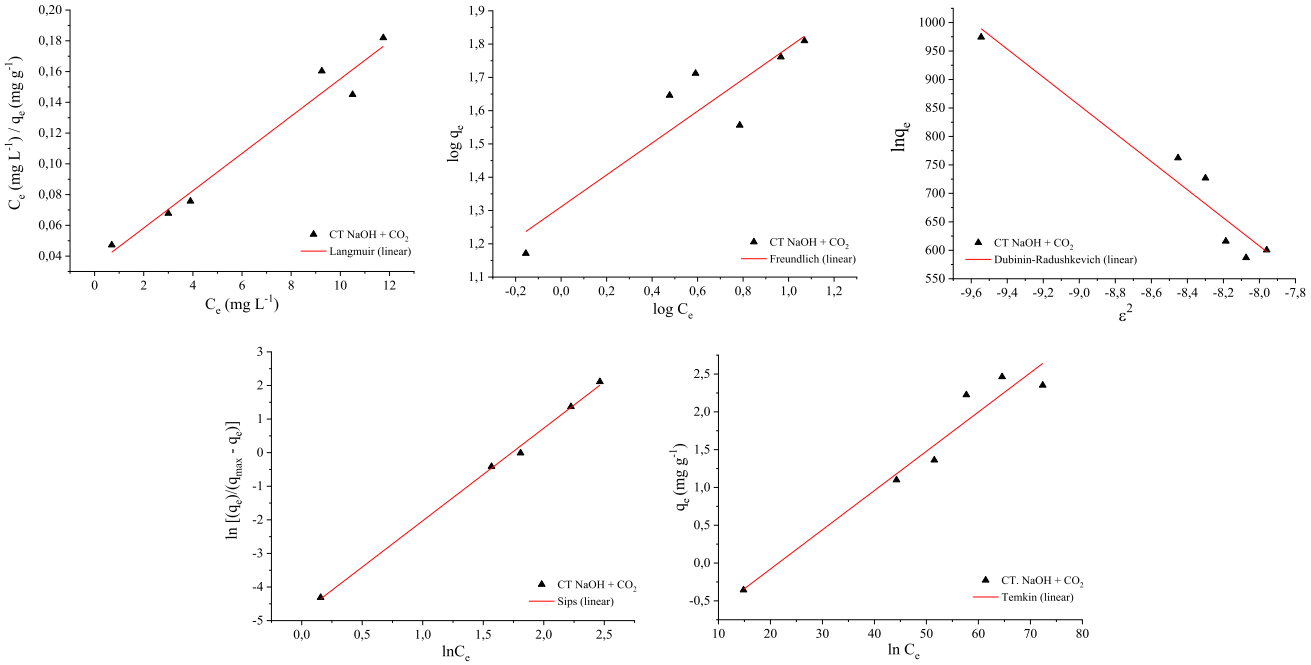

Fig. 8 Langmuir, Freundlich, Dubinin–Radushkevich, Sips, and Temkin linear isotherms (CT NaOH + CO_2 removing Cd^{2+})

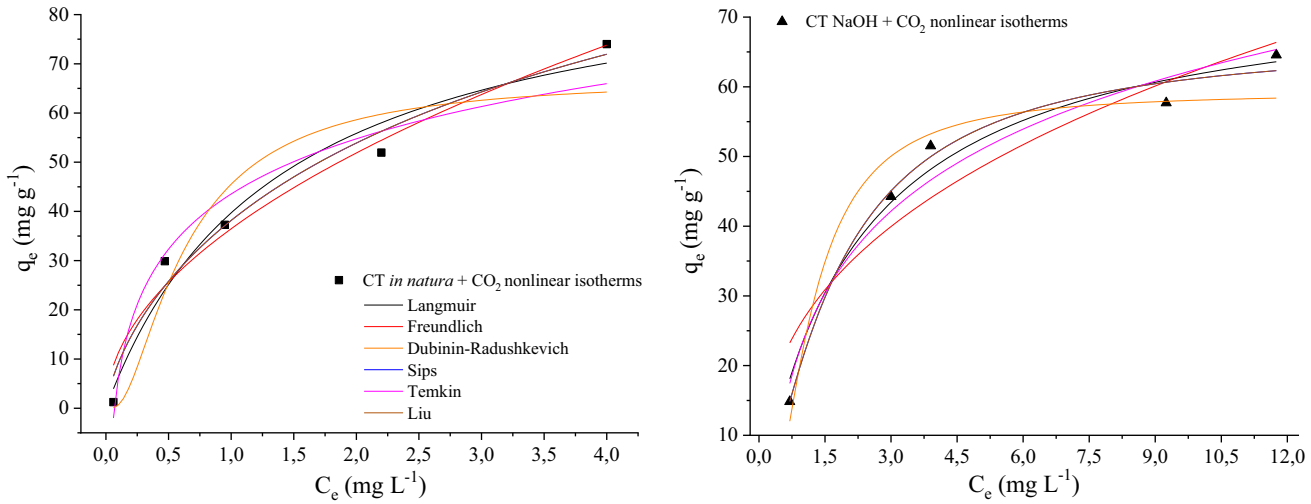

Fig. 9 Non-linear isotherms proposed by Langmuir, Freundlich, Dubinin–Radushkevich, Sips, Temkin, and Liu applied to CT *in natura* + CO_2 and CT NaOH + CO_2 in the removal of Cd^{2+} from water solutions

The K_L values obtained by the linear model of Langmuir are 1.08 L mg^{-1} (CT *in natura* + CO_2) and 0.36 L mg^{-1} (for CT NaOH + CO_2), indicating that the adsorption of Cd^{2+} by CT *in natura* + CO_2 is the result of a more vital interaction between adsorbate/adsorbent. Although with lower values, the estimate of K_L by the non-linear model of Langmuir also shows stronger interactions between CT *in natura* + CO_2 − Cd^{2+} than CT NaOH + CO_2 − Cd^{2+}.

The obtained values for Freundlich are only suitable for CT *in natura* + CO_2, with adj-R^2 values from 0.95 to 0.96 and low values of RRS. The k_f values obtained by the linear model are more suitable for its lower RRS values [k_f linear = 13.51 mg g^{-1} (mg L^{-1})$^{-1/n}$, RRS = 0.049; k_f nonlinear = 36.46 mg g^{-1} (mg L^{-1})$^{-1/n}$], RRS = 3.14).

The n values obtained by Freundlich for CT *in natura* + CO_2 vary from 1.36 to 1.96. According to Taiwo and Chinyere [86], values of n ranging from 1 to 10

Table 5 Parameters for Langmuir, Freundlich, Dubinin–Radushkevich (D-R), Sips, Temkin, and Liu for the removal of Cd^{2+} by CT *in natura* + CO_2 and CT NaOH + CO_2

Parameters	CT *in natura* + CO_2		CT NaOH + CO_2	
Langmuir (linear) $\frac{Ce}{qe} = \frac{1}{qmaxb} + \frac{Ce}{qmax} R_L = \frac{1}{(1+C_0 a)}$		RRS		RRS
q_{max} (mg g^{-1})	76.616	0.004	82.508	0.001
k_L (L mg^{-1})	1.083	0.001	0.356	0.009
$R_{L\ (estimate\ from\ 5\ to\ 300\ mg\ L^{-1})}$	0.208 to 0.940		0.216 to 0.943	
Adj-R^2	0.960		0.956	
Langmuir (non-linear) $q_e = q_{max}\ k_L\ \frac{C_e}{(1+k_L C_e)} R_L = \frac{1}{(1+C_0 k_L)}$				
q_{max} (mg g^{-1})	94.268	14.202	75.638	5.163
k_L (L mg^{-1})	0.727	0.273	0.449	0.104
$R_{L\ (estimate\ from\ 5\ to\ 300\ mg\ L^{-1})}$	0.156 to 0.003		0.009 to 0.359	
Adj-R^2	0.956		0.969	
Freundlich (linear) $\log qeq = \log kf + \left(\frac{1}{n}\right) \log\ Ce$				
k_f[mg g^{-1} (mg $L^{-1})^{-1/n}$]	13.511	0.049	20.464	0.082
n	1.136	0.077	2.087	0.110
1/n	0.880		0.479	
Adj-R^2	0.955		0.782	
Freundlich (non-linear) $q_{eq} = k_f C_{eq}^{\frac{1}{n}}$				
k_f[mg g^{-1} (mg $L^{-1})^{-1/n}$]	36.469	3.143	26.556	5.020
n	1.966	0.296	2.689	0.675
1/n	0.508		0.372	
Adj-R^2	0.958		0.858	
D-R (linear) $\ln qe = \ln Qd - Bd\varepsilon 2$ and $\varepsilon = RT\ln\left(1 + \frac{1}{Ce}\right)$ and $E = \frac{1}{\sqrt{2B_d}}$				
Q_d (mol L^{-1})	0.003	0.229	0.003	0.361
E (KJ mol^{-1})	13.867		11.501	
B_d	0.003	3.1 e^{-4}	0.004	4.9 e^{-4}
Adj-R^2	0.932		0.919	
D-R (non-linear) $q_e = q_{sat}\left(\exp\left(-B_d RTLn\left(1 + \frac{1}{C_e}\right)\right)\right)^2$ and $\varepsilon = RT\ln\left(1 + \frac{1}{Ce}\right)$ and $E = \frac{1}{\sqrt{2B_d}}$				
q_{max} (mg g^{-1})	0.005	0.002	0.005	0.002
E (KJ mol^{-1})	11.656		11.625	
B_d	0.004	5.6 e^{-4}	0.004	5.6 e^{-4}
Adj-R^2	0.957		0.957	
Sips (linear) $\ln\left(\frac{q_e}{q_{max} - q_e}\right) = \frac{1}{n_S}\ln C_e + \frac{1}{n_S}\ln k_S$				
n_S	0.747	0.057	0.363	2.756
k_s (L mg^{-1})	0.856	0.094	0.176	0.078
Adj-R^2	0.993		0.997	
Sips (non-linear) $q_e = q_{sat} k_s C_e^{\left(\frac{n}{1+k_s C_e^{n_S}}\right)}$				
q_{max} (mg g^{-1})	150.038	181.850	78.947	23.005
n_S	0.717	0.411	1.000	0.498
k_s (L mg^{-1})	0.341	0.584	0.389	0.166
Adj-R^2	0.947		0.902	
Temkin (linear) $q_e = B\ lnA_t + B\ln C_e$				
A_t (L mg^{-1})	17.295	0.549	3.536	3.877
b_t	175.050	0.360	135.722	2.137
B (J mol^{-1})	14.154	0.360	18.255	2.137
Adj-R^2	0.997		0.935	

Table 5 (continued)

Parameters	CT *in natura* + CO_2		CT NaOH + CO_2	
Temkin (non-linear) $q_e = \left(\frac{RT}{b_t}\right) \ln\left(A_t C_e\right)$				
A_t (L mg^{-1})	14.742	5.092	3.993	1.244
b_t	153.102	18.874	145.91	15.619
B (J mol^{-1})	16.182		16.979	
Adj-R^2	0.942		0.956	
Liu (non-linear) $q_e = \frac{q_{max}(k_g C_e)^{n_L}}{1+(k_g C_e)^{n_L}}$				
q_{max}	149.922	182.217	74.478	11.564
k_g	0.223	0.720	0.464	0.168
n_L	0.717	0.414	1.231	0.448
Adj-R^2	0.945		0.923	

q_{max}: maximum adsorption capacity; k_L: constant related to adsorbate/adsorbent interaction forces; k_f: related to adsorption capacity; n: related to solid heterogeneity (n for Freundlich and n_S for Sips); Q_d: maximum adsorption capacity; E: average sorption energy; n: related to the heterogeneity of the adsorbent material; ε: the potential of Polanyi; B_d: coefficient related to sorption energy (Dubinin–Radushkevich); k_s is the Sips constant; At (L g^{-1}): Temkin isotherm equilibrium binding constant; b_t: Temkin isotherm constant; B (J mol^{-1}): Constant related to the heat of sorption; k_g: Liu equilibrium constant (L mg^{-1}); n_L: dimensionless exponent of the Liu equation; RSS: residual sum of squares; adj-R^2: adjusted coefficient of determination

suggest favorable conditions to adsorption and a cooperative system, which indicate that there is the reactivity of CT *in natura* + CO_2 active sites with Cd^{2+} in a cooperative manner. According to Al-ghouti and Da'ana [87], when $0 < 1/n < 1$, adsorption is favorable, as shown for all tobacco-ACs (Table 5).

These results above corroborate with our findings already exhibited in Fig. 4, where CT *in natura* + CO_2 exhibit an isotherm (N_2 adsorption/desorption) that indicates the possibility of the formation of multilayer (explained by Freundlich model). In contrast, CT NaOH + CO_2 present an isotherm type I, typical for wmicroporous solids, limited by the formation of a monolayer, explained mainly by Langmuir.

According to Jeppu and Clement [88], the Sips equation offers a flexible analytical framework for modeling both Langmuir and Freundlich type sorption effects. Alyasi et al. [89] state that the Sips behave similarly to the Langmuir isotherm model at high adsorbate concentration but with slightly more significant deviation. The Langmuir isotherm also shows an excellent correlation, although the Sips model is significantly more accurate at the lowest concentrations.

Also known as Langmuir–Freundlich isotherm, the Sips equation is a versatile isotherm expression that can simulate both Langmuir and Freundlich behaviors [88]. In this research, suitable adjustments were obtained by Sips linear equation for CT *in natura* + CO_2 (adj-$R^2 = 0.99$) and NaOH + CO_2 (adj-$R^2 = 0.99$), which can suggest the occurrence of mono and multilayer of Cd^{2+} adsorption by the tobacco-ACs.

Also, if the value of $n_S = 1$, that means that the adsorbent material is entirely homogeneous, whereas values of n_S closer to 0 suggest heterogeneous materials. Mathematically, when $n_S = 1$, the Sips isotherm is reduced to the Langmuir isotherm, i.e., predicts predominant monolayer adsorption [89]. By the linear equation of Sips, it can be seen that the tobacco adsorbents exhibit values of $n_S = 0.74$ (CT *in natura* + CO_2 and 0.36 (CT NaOH + CO_2), suggesting that the Cd^{2+} adsorption processes are not exclusively governed by the two-parameter Langmuir isotherm [90].

Good adjustments were also found for Dubinin–Radushkevich nonlinear equation for CT *in natura* + CO_2 (adj-$R^2 = 0.96$) and CT NaOH + CO_2 (0.96). It is observed in Table 5 that E (sorption energy) assume values of 11.65 kJ mol^{-1} (CT *in natura* + CO_2) and 11.62 kJ mol^{-1} (CT NaOH + CO_2), which according to the interpretation of Gonçalves Jr et al. [80] $E > 8$ kJ mol^{-1} suggests the occurrence of chemisorption. However, recent studies[77, 91] state that the use of the D–R isotherm model to describe the adsorption of a solute at the solid/solution interface is different from its use in gas adsorption (which D-R was initially designed for). According to them, the D-R model ignores the influence of the solvent, solution pH, the chemical species of the solutes, surface charge, and functional groups dissociation of the adsorbents in a solid/solution adsorption system. So, D–R isotherm may not accurately provide the average free energy to distinguish physical or chemical adsorption

in a solid/solution adsorption system. The assumptions of Temkin isotherm are (i) the adsorption heat of the surface molecules decreases linearly rather than logarithmically with coverage; (ii) the adsorption process is characterized by a uniform distribution of binding energies at the adsorbent surface; and (iii) this model covers the adsorbate-adsorbent interaction [63, 84]. In our research, suitable adjustments were found by applying Temkin linear isotherm for Cd^{2+} adsorption by CT *in natura* + CO_2.

The slightly better adjustment of Temkin linear isotherm for CT NaOH + CO_2 (adj-R2 = 0.96) than CT *in natura* + CO_2 (adj-R^2 = 0.94) can imply that Cd^{2+} adsorption process by CT NaOH + CO_2 is more likely to be affected by the sorbate/sorbent interaction. Similar results were found by Tian et al. [84] by using sludge-derived char for Pb^{2+} and Cd^{2+} removal from waters.

A_t (ranging from 3.87 to 17.29 L mg^{-1}) is the equilibrium binding constant, which indicates the maximum bonding energy, whereas the B constant is related to the heat of adsorption (values ranging from 14.15 to 16.97 J mol^{-1}). When B > 0, it indicates an exothermic process [53], as observed for the adsorption of Cd^{2+} by both tobacco-ACs. According to Nascimento et al. [63], the heat involved in the physisorption is generally below 10 kcal mol^{-1}, i.e., on the order of condensation/vaporization. In chemical adsorption, the heat of adsorption is of the order of reaction heat, so above 20 kcal mol^{-1}. In this sense, B values assume values from 3.38 cal mol^{-1} to 4.3 cal mol^{-1}, i.e., the estimated adsorption heat is deficient, suggesting the predominance of physical forces in the Cd^{2+} sorption, such as Wan der Waals forces and other intermolecular forces.

Reasonable adjustment was found by Liu isotherm for CT *in natura* + CO_2 (adj-R^2 = 0.94) and CT NaOH + CO_2 (adj-R^2 = 0.92), with respectively values of q_{max} of 149.92 mg g^{-1} (in this case with high RRS = 182.217) and 74.48 mg g^{-1} (RRS = 11.564).

Like Sips, the Liu model combines the Langmuir and Freundlich isotherm models, but in this case, the monolayer assumption of the Langmuir model and the infinite adsorption assumption originates from the Freundlich model is discarded [92]. Liu isotherm predicts that the active sites of the adsorbent cannot possess the same energy [52].

Prola et al. [93] found out that the Liu model can present RRS values lower than Langmuir, Freundlich, and Sips models, indicating that this isotherm model was a better fit the experimental equilibrium data. Also, Lima et al. [92] state that the advantages of the Liu isotherm model (a 3-parameter isotherm) over the Sips isotherm model is that the exponent of Liu isotherm could admit any positive value, unlike the exponent of Sips that is limited to $1/n \leq 1$.

Based on the obtained values of q_{max} and k_f, our tobacco-based AC is superior (in terms of Cd^{2+} uptake) to grape stem biosorbent [56], AC from *Ulva Lactuca* [74], AC from oak wood [94], carbon activated with rhamnolipid biosurfactant [95], having a similar capacity than the composite AC (carbon/zirconium oxide) [96] (Table 6).

Table 6 Comparison among tobacco activated carbons (ACs) and other materials in terms of Cd^{2+} removal rates

Adsorbent	q_{max} (Langmuir) (mg g^{-1})	k_f (Freundlich) [mg g^{-1} (mg $L^{-1})^{-1/n}$]	Linear or nonlinear	Contaminant	Reference
CT *in natura* + CO_2 AC	94.27	36.47	Non-linear	Cd^{2+}	This research
CT NaOH + CO_2 AC	75.64	26.56	Non-linear	Cd^{2+}	This research
Ulva Lactuca AC	84.60	–	–	Cd^{2+}	Ibrahim, Hassan and Azab [74]
Grape stem biosorbent activated with NaOH	14.92	7.79	Linear	Cd^{2+}	Schwantes et al. [55–57]
AC from tobacco ($ZnCl_2$)	84.75	7.16	Linear	Pb^{2+}	Conradi Jr. et al. [27]
Oak wood AC	4.34	3.72	Linear	Cd^{2+}	Hajati, Ghaedi and Yaghoubi [94]
AC/ zirconium oxide composite	166.7	16.59	–	Cd^{2+}	Sharma and Naushad [96]
AC from *Nigella sativa* seeds	18.16	50.30	Non-linear	Cd^{2+}	Thabede et al. [97]
AC activated by rhamnolipid biosurfactant	50.00	19.76	Non-linear	Cd^{2+}	Shami, Shojaei and Khoshdast [95]
Biogenic Ag@Fe nanocomposite adsorbent	125.00	15.80	Non-linear	Methyl red	Zaheer, Al-Asfar and Aazam [98]
Silver impregnated AC	2.65	1.62	Linear	Cr(VI)	Mishra and Ghosh [99]
Spirulina/chitosan foam	–	0.101	Non-linear	Phenol	Alves et al. [100]
Soil—Rhodic Ferralsol (mainly hematite)	389.61	2.03	Non-linear	Chlorpyrifos	Schwantes et al. [7]

AC activated carbon

The order for the best adjustments found using nonlinear models in the adsorption of Cd^{2+} by CT *in natura* + CO_2 was: Freundlich > D-R > Langmuir > Sips > Liu > Temkin; for nonlinear models applied on CT NaOH + CO_2: Langmuir > D-R > Temkin > Liu > Sips > Freundlich. For the use of linear models, for CT *in natura* + CO_2 we have the following order: Temkin > Sips > Langmuir > Freundlich > D-R; and for CT NaOH + CO_2: Sips > Langmuir > Temkin > D-R > Freundlich.

The results above suggest that no single ruler governs the uptake of Cd^{2+} by the tobacco-ACs (chemical bonds or weak physical interactions, specific surface group, etc.), but a diversity of factors that possibly rule the removal of Cd^{2+} from solution. According to Schwantes et al. [7], this usually occurs when studying complex and heterogeneous matrices, such as the colloidal interfaces of soils or biomasses (such as ACs). Those materials have complex and heterogeneous surfaces (Fig. 2, and there is more than one type of interaction (physical and chemical; strong and weak, etc. among the active sites and the Cd^{2+} ions. Thus, the removal of Cd^{2+} occurs through a set of interactions between adsorbent/adsorbate.

In almost every adsorption study, linear shapes have been used to conclude the best kinetic/equilibrium model that influences the adsorption mechanism. This result can be a mistake because, in some instances, as found in some of our findings, even with some relatively high errors, the mathematical adjustments are superior for non-linear models, suggesting better adequacy of experimental data [101]. Many authors observed that non-linear models have a better fit to the experimental data, like Sahin and Tapadia [102], by evaluating fluoride adsorption onto a limonite geo-material,or like Markandeya et al. [103], by evaluating disperse orange 25 dye on AC; or even like Can [104], by studying rhodium adsorption onto gallic acid derived polymer,or Moussout et al. [81], which studied Cd^{2+} adsorption onto chitosan (Cd^{2+}/CS) and methyl orange onto bentonite (MO/Bt).

The parameter values estimated by linear isotherms are relatively different from those observed by non-linear equations; for example, high values for adj-R^2 are sometimes accompanied by high RRS values and overestimated parameters, with discrepancies between the calculated and estimated values and q_{max} (Table 5). According to Moussout [81], non-linear regression is a more general method that can be used to estimate the parameters of empirical mathematical models. Its main advantage is the easy adjustment, even if the isotherm model cannot be linearized. In addition, the linearization process modifies the original equations, which may cause some variation in the final result, not corresponding with the observed natural phenomena [105]. Thus, the use of non-linear models may help interpret the obtained results by linearizations or, on the other hand, may demonstrate when the linearized parameters have misleading results [106].

The mathematical reason for differences between linear and non-linear models is that linear regression considers the standard deviation equally at each point. However, due to linearization, the unit standard deviation at each point in the linear form is not valid for the non-linear form [105].

Desorption studies and the reuse of the tobacco activated carbons (acid elution desorption)

In order to determine the possibility of reuse of ACs, the isotherm construction was followed by the recovery of the ACs and the desorption evaluation in acid elution (HCl 0.1 mol L^{-1}). The following Cd^{2+} desorption rates were obtained:

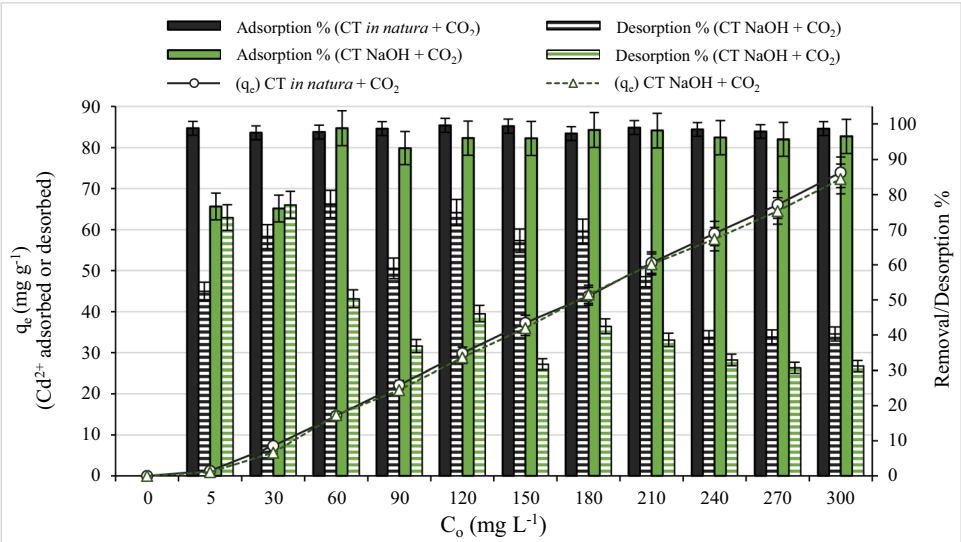

Fig. 10 Adsorption *versus* desorption % of Cd^{2+} by the tobacco activated carbons (CT *in natura* + CO_2 and CT NaOH + CO_2)

CT *in natura* + CO_2 58.52% and CT NaOH + CO_2 44.64% (Fig. 10).

The non-desorbed portion (41.48% for CT *in natura* + CO_2; 55.36% for CT NaOH + CO_2) may indicate that some of the Cd^{2+} were chemically adsorbed to the carbon structure. Thus, chemical bonds could be ruling Cd^{2+} adsorption, as already predicted by pseudo-second order (high adj-R^2 and low RRS) and Langmuir (high adj-R^2 and low RRS), which suggest that at least part of the observed adsorption is ruled by the chemical affinity between adsorbent/adsorbate. Nevertheless, the excellent desorption rates observed for both ACs (58.52% for CT *in natura* + CO_2 and 44.64% for CT NaOH + CO_2) also suggests that a significant part of the Cd^{2+} uptake is physically retained, i.e., this result highlight the reversibility of the adsorption reaction, suggesting that Cd^{2+} is mostly physisorbed (dipole-diploe forces, ion–dipole forces or London dispersion forces) [107, 108]. These results corroborate with what was already highlighted by the goodness of the fit found and the interpretation of the parameters from pseudo-first order (high adj-R^2 and low RRS), Freundlich (high adj-R^2 and low RRS), Sips (high adj-R^2; low RRS and $n_S < 1$) and Temkin (high adj-R^2, low RRS and B < 20 kcal mol^{-1}).

Similar results are found in the literature by Coelho et al. [109], where using biosorbent from *Anacardium occidentale* L. the authors found 56% of Cd^{2+} of desorption (unmodified biosorbent), 50% (biosorbent modified with H_2O_2 1 mol L^{-1}), 97% (biosorbent modified with H_2SO_4 1 mol L^{-1}) and 77% (biosorbent modified with NaOH). Gonçalves Jr. et al. [80] by using açaí berry biosorbent found out 44.5% of Cd^{2+} desorption. It is essential to highlight that both authors used an acid elution of HCl 0.1 mol L^{-1} for their evaluations, using a similar desorption method to ours (acid elution).

As the produced ACs have as precursor raw-material the tobacco, the adsorbents resulting from the triple (thermal-chemical-physical) and double (thermal-physical) activation have small concentrations of Cd, Pb, and Pb in their composition Cr. As Table 1 show, CT *in natura* + CO_2 contains 20 mg kg^{-1} of Cd, 61 mg kg^{-1} of Pb and 25.00 mg kg^{-1} of Cr, while CT NaOH + CO_2 contains 4 mg kg^{-1} of Cd, 90 mg kg^{-1} of Pb, and 36 mg kg^{-1} of Cr.

In order to evaluate the possibility of releasing some trace concentration of Cd, Pb, or Cr into the water solution in extreme conditions, the ACs (before any adsorption study) were set in contact (200 mg) with 50 mL of HCl 0.1 mol L^{-1}, and stirred for 1.5 h. As a result, no Pb or Cr was detected in the water solution, but 0.076 mg L^{-1} of Cd^{2+} was found out.

Moreover, desorption tests with water (at pH 7.0, in the same conditions above) were conducted to simulate the possible Cd^{2+}releasing into water. As a result no Pb or Cr was detected in the water solution, but trace Cd^{2+} concentrations were found: CT *in natura* + CO_2 = 0.013 mg L^{-1}; CT NaOH + CO_2 = < 0.005 (LQ). It is important to state that this amount of Cd^{2+} ($[Cd^{2+}]_{HCl}$ 0.076 mg L^{-1}; $[Cd^{2+}]_{water}$ 0.013 mg L^{-1}) complies with the provisions of CONAMA 430/2011 [110] but does not fall within limits established by Resolution 2914/Ministry of Health [111] ($[Cd^{2+}]$ maximum permitted value = 0.005 mg L^{-1}), which concerns the human consumption of freshwater. Considering those above, as a matter of safety, we recommend the use of the developed ACs as part of the water/wastewater industrial treatment systems, and we also state that it is advisable to add a component after the use of AC in order to remove eventual trace concentrations of Cd^{2+} from water.

Adsorption thermodynamics

The results found out by the evaluation of the thermodynamics of Cd^{2+} adsorption by CT *in natura* + CO_2, and CT NaOH + CO_2 (Table 7) suggests that the uptake of Cd^{2+} is exothermic ($\Delta H°_{\text{CT } in\ natura\ +\ CO2} = -14.75$ kJ mol^{-1}; $\Delta H°_{\text{CT NaOH } +\ CO2} = -16.92$ kJ mol^{-1}) [112]. The $\Delta H° < 40$ kJ mol^{-1} may indicate the predominance of physisorption of Cd^{2+} by the tobacco adsorbents, with adsorption of Cd^{2+} by the surface functional groups (Fig. 3) that may act a fundamental role in the colloidal interface, such

Table 7 Thermodynamics parameters for CT *in natura* + CO_2 and CT NaOH + CO_2 in the removal of Cd^{2+}

Activated carbon (AC)	Temp (°C)	q_e (mg g^{-1})	$\Delta G°$ (KJ mol^{-1})	$\Delta H°$ (KJ mol^{-1})	$\Delta S°$ (J mol^{-1})	R^2
CT *in natura* + CO_2	15	12.460 ± 0.28	− 19.557 ± 0.11	− 14.749 ± 3.58	16.695 ± 3.54	0.636
	25	12.418 ± 0.21	− 19.724 ± 0.16			
	35	12.408 ± 0.35	− 19.891 ± 0.29			
	45	12.390 ± 0.23	− 20.058 ± 0.28			
	55	12.400 ± 0.12	− 20.225 ± 0.19			
CT NaOH + CO_2	15	12.444 ± 0.38	− 43.329 ± 0.27	− 16.917 ± 2.35	91.708 ± 2.89	0.692
	25	12.457 ± 0.22	− 44.247 ± 0.19			
	35	12.447 ± 0.28	− 45.164 ± 0.11			
	45	12.477 ± 0.24	− 46.081 ± 0.20			
	55	12.474 ± 0.36	− 46.998 ± 0.17			

as COO–, C–O, C–O–C, C=O, and O–H. The values of $\Delta G° < 0$ (Table 7) indicate that the observed adsorption phenomenon is an energetically favorable and spontaneous process (at the studied range of temperatures from 25 to 35 °C) [113].

Conclusion

The obtained results demonstrate that the proposed method of producing AC (by thermal-chemical activation and by thermal-chemical-physical activation) is feasible (yield of 43% for CT *in natura* + CO_2 and 58% CT NaOH + CO_2), generating adsorbents with a high Cd^{2+} adsorption capacity for possible application in water and wastewater treatment systems.

The developed tobacco-based adsorbents are gifted with high pH_{PZC} values (CT *in natura* + CO_2 = 11.11 and CT NaOH + CO_2 = 10.86) due to the generation of carbonaceous groups on the surface and the physical activation with CO_2. SEM analysis shows heterogeneous morphologies and an irregular surface; FT-IR analysis evidence the surface functional groups COO–, C–O, C–O–C, C=O, and O–H, possibly from carboxylic acids, hydroxyl, esters, ketones, and aldehydes. BET analysis shows a specific surface area of 2.30 g m^{-2} (CT *in natura* + CO_2) and 103.40 g m^{-2} (CT NaOH + CO_2), which indicate excellent adsorptive properties.

The optimal conditions for adsorption were found out by using 4.0 g L^{-1} of activated carbon, regardless of the evaluated pH value (studied range: 3.0 to 7.0); the Cd^{2+} uptake is a fast process, with most of the metal adsorbed in the first 10–20 min of contact time; and the uptake of Cd^{2+} by tobacco adsorbents is exothermic ($\Delta H° < 0$), is constituted of an energetically favorable and spontaneous process ($\Delta G° < 0$).

Considering: 1st) the goodness of the fit (high adj-R^2 and low RRS) found for pseudo-first-order, pseudo-second order, intraparticle diffusion, Langmuir, Freundlich, Dubinin–Radushkevich, Sips, Temkin and Liu; 2nd) the surface groups COO–, C–O, C–O–C, C=O, and O–H; 3rd) the pH_{PZC} values (CT *in natura* + CO_2 = 11.11 and CT NaOH + CO_2 = 10.86); 4th) the heterogeneous and irregular structures highlighted by SEM micrographs; 5th) the enhanced SSA evidenced by N_2 adsorption/desorption isotherms (CT *in natura* + CO_2 = 2.30 g m^{-2} and CT NaOH + CO_2 = 103.40 g m^{-2}); 6th) $\Delta H° < 0$ kJ mol^{-1} and the considerable desorption rates (desorption of 58.52% for CT *in natura* + CO_2 and 44.64% for CT NaOH + CO_2) it is possible to state that the Cd^{2+} uptake by tobacco activated carbons is a complex process, not ruled by a single factor. Thus, Cd^{2+} removal seems to occur by chemisorption and physisorption, with the formation of mono and multilayers. Also, the values of $\Delta G° < 0$ kJ mol^{-1} indicate that the observed phenomena are an energetically favorable and spontaneous process; and the values of $\Delta H° < 0$ and the effective desorption rates suggest that the adsorption of Cd^{2+} is ruled mainly (but not only) by physical interactions between adsorbent/adsorbate.

Thus, tobacco use as a raw material for activated carbon development is a renewable and eco-friendly technique, especially for smuggled cigarettes, such as those seized between Brazil and Paraguay.

Supplementary Information The online version contains supplementary material available at https://doi.org/10.1007/s40201-021-00740-8.

Acknowledgements Financial support: Federal Justice of Paraná and CNPq. This study was financed in part by the Coordenação de Aperfeiçoamento de Pessoal de Nível Superior—Brasil (CAPES)—Finance Code 001. Especial thanks to the Universidade Estadual de Londrina (UEL) for conducting the FT-IR and SEM analyses.

Declarations

Conflict of interest The authors declare that they have no known competing financial interests or personal relationships that could have appeared to influence the work reported in this paper.

References

1. FAO. Food and agriculture data—world population. Food and agriculture organization of the United Nations. 2017. http://www.fao.org/faostat/en/. Accessed 01 May 2020.
2. Gonçalves AC Jr, Schwantes D, de Sousa RFB, Da Silva TRB, Guimarães VF, Campagnolo MA, De Vasconcelos ES, Zimmermann J. Phytoremediation capacity, growth and physiological responses of *Crambe abyssinica* Hochst on soil contaminated with Cd and Pb. J Environ Manag. 2020;262:110342. https://doi.org/10.1016/j.jenvman.2020.110342.
3. Zhou Q, Yang N, Youzhi L, Ren B, Ding X, Hualin B, Yao X. Total concentrations and sources of heavy metal pollution in global river and lake water bodies from 1972 to 2017. Glob Ecol Conserv. 2020;22:e00925. https://doi.org/10.1016/j.gecco.2020.e00925.
4. Schwantes D, Gonçalves AC Jr, Manfrin J, Campagnolo MA, Zimmermann J, Conradi Junior E, Bertoldo DC. Distribution of heavy metals in sediments and their bioaccumulation on benthic macroinvertebrates in a tropical Brazilian watershed. Ecoleng. 2021;163:106194. https://doi.org/10.1016/j.ecoleng.2021.106194.
5. Ghazy HA, Abdel-Razek MAS, Nahas AFE, Mahmoud S. Assessment of complex water pollution with heavy metals and pyrethroid pesticides on transcript levels of metallothionein and immune related genes. Fish Shellfish Immunol. 2017;68:318–26. https://doi.org/10.1016/j.fsi.2017.07.034.
6. Polidoro BA, Comeros-Raynal MT, Cahill T, Clement C. Land-based sources of marine pollution: pesticides, PAHs and phthalates in coastal stream water, and heavy metals in coastal stream sediments in American Samoa. Mar Pollut Bull. 2017;116(1–2):501–7. https://doi.org/10.1016/j.marpolbul.2016.12.058.
7. Schwantes D, Gonçalves AC Jr, Conradi Junior E, Campagnolo MA, Zimmermann J. Determination of CHLORPYRIFOS by

GC/ECD in water and its sorption mechanism study in a RHODIC FERRALSOL. J Environ Health Sci Eng. 2020. https://doi.org/10.1007/s40201-020-00448-1.
8. Chen H, Ye J, Zhou Y, Wang Z, Jia Q, Nie Y, Li L, Liu H, Benoit G. Variations in CH4 and CO2 productions and emissions driven by pollution sources in municipal sewers: an assessment of the role of dissolved organic matter components and microbiota. Environ Pollut. 2020;263:114489. https://doi.org/10.1016/j.envpol.2020.114489.
9. Khdair AI, Abu-Rumman G, Khdair SI. Pollution estimation from olive mills wastewater in Jordan. Heliyon. 2019;5(8):e02386. https://doi.org/10.1016/j.heliyon.2019.e02386.
10. Manfrin J, Schwantes D, Gonçalves AC Jr, Ferronato MC, Aleixo V, Schiller AP. Contamination by lead in sediments at Toledo River, hydrographic basin of PARANÁ III. Environ Monit Assess. 2018;190:243. https://doi.org/10.1007/s10661-018-6611-9.
11. Manfrin J, Schwantes D, Gonçalves AC Jr, Schiller AP, Zimmerman J, de Oliveira VHD. Evaluation of benthic macroinvertebrates as indicators of metal pollution in Brazilian rivers. Int J River Basin Manag. 2019. https://doi.org/10.1080/15715124.2019.1628032.
12. Schiller AP, Ferronato MC, Schwantes D, Gonçalves AC Jr, Barilli D, Manfrin J. Influence of hydrological flows from tropical watersheds on the dynamics of Cu and Zn in sediments. Environ Monit Assess. 2019;191:86. https://doi.org/10.1007/s10661-019-7193-x.
13. Schwantes D, Gonçalves AC Jr, Schiller AP, Manfrin J, Campagnolo MA, Somavilla E. *Pistia stratiotes* in the phytoremediation and post-treatment of domestic sewage. Int J Phytoremediat. 2019;21(7):714–23. https://doi.org/10.1080/15226514.2018.1556591.
14. ATSDR. ATSDR's Substance Priority List. Agency for toxic substances & disease registry. 2019. https://www.atsdr.cdc.gov/spl/index.html. Accessed 15 Mar 2020.
15. Kubier A, Wilkin RT, Pichler T. Cadmium in soils and groundwater: a review. Appl Geochem. 2019;108:104388. https://doi.org/10.1016/j.apgeochem.2019.104388.
16. Hamid Y, Tang L, Sohail MI, Cao X, Hussain B, Aziz MZ, Usman M, He Z-L, Yang X. An explanation of soil amendments to reduce cadmium phytoavailability and transfer to food chain. Sci Total Environ. 2019;660:80–96. https://doi.org/10.1016/j.scitotenv.2018.12.419.
17. Đukić-Ćosić D, Baralić K, Javorac D, Đorđević AB, Bulat Z. An overview of molecular mechanisms in cadmium toxicity. Curr Opin Toxicol. 2020;19:56–62. https://doi.org/10.1016/j.cotox.2019.12.002.
18. ATSDR. Cadmium. Agency for Toxic Substances & Disease Registry. 2020. https://www.atsdr.cdc.gov/substances/toxsubstance.asp?toxid=15. Accessed 15 Mar 2020.
19. CETESB - Companhia Ambiental do Estado De São Paulo. Ficha de Informação Toxicológica: Cádmio e seus compostos. São Paulo: CETESB, 2012. http://laboratorios.cetesb.sp.gov.br/wp-content/uploads/sites/47/2013/11/cadmio.pdf. Accessed 15 Mar 2020.
20. International Programme on Chemical Safety. Executive Board. International Programme on Chemical Safety (IPCS). World Health Organization. 1992;89. https://apps.who.int/iris/handle/10665/170790. Accessed 15 Mar 2020.
21. WHO. World Health Organization: Guidelines for drinking-water quality. 4th edition. 2017. https://www.who.int/publications/i/item/9789241549950. Accessed 15 Mar 2020.
22. WHO. World Health Organization: Exposure to cadmium—a major public health concern. Switzerland, 2010. http://www.who.int/ipcs/features/cadmium.pdf. Accessed 15 Mar 2020.
23. Zhang H, Reynolds M. Cadmium exposure in living organisms: a short review. Sci Total Environ. 2019;678:761–7. https://doi.org/10.1016/j.scitotenv.2019.04.395.
24. Tolcin AC. Cadmium: 2015 minerals yearbook. New York: U.S.S Department of the Interior. 1. ed. 2015. https://minerals.usgs.gov/minerals/pubs/commodity/cadmium/myb1-2015-cadmi.pdf. Accessed 15 Mar 2020.
25. Hokkanen S, Bhatnagar A, Sillanpää M. A review on modification methods to cellulose-based adsorbents to improve adsorption capacity. Water Res. 2016;91:156–73. https://doi.org/10.1016/j.watres.2016.01.008.
26. Masoumi S, Dalai AK. Optimized production and characterization of highly porous activated carbon from algal-derived hydrochar. J Clean Prod. 2020;263:121427. https://doi.org/10.1016/j.jclepro.2020.121427.
27. Conradi E Jr, Gonçalves AC Jr, Schwantes D, Manfrin J, Schiller A, Zimmermann J, Klassen GJ, Ziemer GL. Development of renewable adsorbent from cigarettes for lead removal from water. J Environ Chem Eng. 2019;7(4):103200. https://doi.org/10.1016/j.jece.2019.103200.
28. Agência Brasil. Comércio ilegal de cigarros supera mercado regular no Brasil. 2018. http://agenciabrasil.ebc.com.br/economia/noticia/2018-11/comercio-ilegal-de-cigarros-supera-mercado-regular-nobrasil/. Accessed 15 May 2020.
29. Manfrin J, GonçalvesJr AC, Schwantes D, Conradi E Jr, Zimmermann J, Ziemer GL. Development of biochar and activated carbon from cigarettes wastes and their applications in Pb^{2+} adsorption. J Environ Chem Eng. 2021;9:104980. https://doi.org/10.1016/j.jece.2020.104980.
30. Manfrin J, Gonçalves AC Jr, Schwantes D, Tarley CRT, Schiller AP, Klassen GJ. Triple activation (thermal-chemical-physical) in the development of an activated carbon from tobacco: characterizations and optimal conditions for Cd^{2+} and Pb^{2+} removal from waters. Water Pract Technol. 2020;15(4):877–98. https://doi.org/10.2166/wpt.2020.069.
31. Ghadiri SK, Alidadi H, Nezhad NT, Javid A, Roudbari A, Talebi SS, Mohammadi AA, Shams M, Rezania S. Valorization of biomass into amine- functionalized bio graphene for efficient ciprofloxacin adsorption in water-modeling and optimization study. Plos One. 2020. https://doi.org/10.1371/journal.pone.0231045.
32. Gholami Z, Ghadiri SK, Avazpour M, Fard MA, Yousefi N, Talebi SS, Khazaei M, Saghi MH, Mahvi AH. Removal of phosphate from aqueous solutions using modified activatedcarbon prepared from agricultural waste (*Populous caspica*): optimization, kinetic, isotherm, and thermodynamic studies. Desalin Water Treat. 2018;133:177–90. https://doi.org/10.5004/dwt.2018.23000.
33. Haghighat GA, Sadeghi S, Saghi MH, Ghadiri SK, Anastopoulos I, Giannakoudakis DA, Colmenares JC, Shams M. Zeolitic imidazolate frameworks (ZIFs) of various morphologies against eriochrome black-T (EBT): optimizing the key physicochemical features by process modeling. Colloids Surf A Physicochem Eng Asp. 2020;606:125391. https://doi.org/10.1016/j.colsurfa.2020.125391.
34. Haghighat GA, Saghi MH, Anastopoulos I, Javid A, Roudbari A, Talebi SS, Ghadiri SK, Giannakoudakis DA, Shams M. Aminated graphitic carbon derived from corn stover biomass as adsorbent against antibiotic tetracycline: optimizing the physicochemical parameters. J Mol Liq. 2020;313:113523. https://doi.org/10.1016/j.molliq.2020.113523.
35. Jahangiri K, Yousefi N, Ghadiri SK, Fekri R, Bagheri A, Talebi SS. Enhancement adsorption of hexavalent chromium onto modified fly ash from aqueous solution; optimization; isotherm, kinetic and thermodynamic study. J Disper Sci Technol. 2018;40(8):1147–58. https://doi.org/10.1080/01932691.2018.1496841.
36. Javid A, Roudbari A, Yousefi N, Fard MA, Barkdoll B, Talebi SS, Nazemi S, Ghanbarian M, Ghadiri SK. Modeling of chromium (VI) removal from aqueous solution using modified

green-graphene: RSM-CCD approach, optimization, isotherm, and kinetic studies. J Environ Health Sci Eng. 2020;18:515–29. https://doi.org/10.1007/s40201-020-00479-8.
37. Sadeghi S, Zakeri HR, Saghi MH, Ghadiri SK, Talebi SS, Shams M, Dotto GL. Modified wheat straw–derived graphene for the removal of eriochrome black T: characterization, isotherm, and kinetic studies. Environ Sci Pollut Res. 2021;28:3556–65. https://doi.org/10.1007/s11356-020-10647-w.
38. Yin Z, Xu S, Liu S, Xu S, Li J, Zhang Y. A novel magnetic biochar prepared by K2FeO4-promoted oxidative pyrolysis of pomelo peel for adsorption of hexavalent chromium. Bioresour Technol. 2020;300:122680. https://doi.org/10.1016/j.biortech.2019.122680.
39. Kim D-W, Wee J-H, Yang C-M, Yang KS. Efficient removals of Hg and Cd in aqueous solution through NaOH-modified activated carbon fiber. Chem Eng J. 2020;192:123768. https://doi.org/10.1016/j.cej.2019.123768.
40. Latimer GW. Official Methods of Analysis of A.O.A.C. International. 21st ed. Association of Official Agricultural Chemists: Maryland; 2012.
41. Welz B, Sperling M. Atomic absorption spectrometry. 3rd ed. Weinheim: Wiley-VCH; 2008.
42. Barros NB, Bruns RE, Scarminio IS. How do experiments: applications in science and industry. 4th ed. Nova Iorque: Bookman; 2010.
43. Lagergren S. Zur theorie der sogenannten adsorption geloster stoffe. Kungliga Svenska Vetenskapsakademiens Handlingar. 1898;24(4):1–39.
44. Ho YS, Mckay G. A kinetic study of dye sorption by biosorbent waste product pith. Resour Conserv Recycl. 1999;25:171–93. https://doi.org/10.1016/S0921-3449(98)00053-6.
45. Roginski SZ. Adsorption and catalysis on inhomogeneous surfaces. Moscow: Izdatelstvo AN SSSR; 1948. p. 353–455.
46. Weber WJ, Morris JC. Kinetics of adsorption on carbon from solution. J Sanit Eng Divis ASCE. 1963;89(2):31–60.
47. Langmuir I. The constitution and fundamental properties of solids and liquids. J Am Chem Soc. 1916;38(11):2221–95. https://doi.org/10.1021/ja02268a002.
48. Freundlich HMF. Over the adsorption in solution. J Phys Chem. 1906;657:385–471.
49. Dubinin MM, Radushkevich LV. The equation of the characteristic curve of the activated charcoal, Proceedings of the National Academy of Sciences. USSR Phys Chem Sect. 1947;55:331–7.
50. Sips R. Combined form of Langmuir and Freundlich equations. J Chem Phys. 1948;16:490–5.
51. Temkin MI, Pyzhev V. Kinetics of ammonia synthesis on promoted iron catalyst, acta physiochim. URSS. 1940;12:327–56.
52. Liu Y, Xu H, Yang S-F, Tay J-H. A general model for biosorption of Cd^{2+}, Cu^{2+} and Zn^{2+} by aerobic granules. J Biotechnol. 2003;102:233–9. https://doi.org/10.1016/S0168-1656(03)00030-0.
53. Pongener C, Bhomich PC, Supong A, Baruah M, Ub S, Sinha D. Adsorption of fluoride onto activated carbon synthesized from *Manihot esculenta* biomass—equilibrium, kinetic and thermodynamic studies. J Environ Chem Eng. 2018;6(2):2382–9. https://doi.org/10.1016/j.jece.2018.02.045.
54. Li L, Jia C, Zhu X, Zhang S. Utilization of cigarette butt waste as functional carbon precursor for supercapacitors and adsorbents. J Clean Prod. 2020;256:120326. https://doi.org/10.1016/j.jclepro.2020.120326.
55. Schwantes D, Gonçalves AC, Campagnolo MA, Tarley CRT, Dragunski DC, Manfrin J, Schiller ADP. Use of co-products from the processing of cassava for the development of adsorbent materials aiming metal removal. In: Waisundara V, editor. Cassava. London: InTech; 2018. p. 265–90.
56. Schwantes D, Gonçalves AC Jr, Campagnolo MA, Tarley CRT, Dragunski DC, de Varennes A, Silva AKS, Conradi E Jr. Chemical modifications on pinus bark for adsorption of toxic metals. J Environ Chem Eng. 2018;6(1):1271–8. https://doi.org/10.1016/j.jece.2018.01.044.
57. Schwantes D, Gonçalves AC Jr, De Varennes A, Braccini AL. Modified grape stem as a renewable adsorbent for cadmium removal. Water Sci Technol. 2018;78(11):2308–20. https://doi.org/10.2166/wst.2018.511.
58. Overend RP, Milne TA, Mudge LK. Fundamentals of thermochemical biomass conversion. Dordrecht: Springer Netherlands; 1985. https://doi.org/10.1007/978-94-009-4932-4.
59. Pezoti O, Cazzeta AL, Bedin KC, Souza LS, Martins AC, Silva TL, Santos Júnior OO, Visentainer JV, Almeida VC. NaOH-activated carbon of high surface area produced from guava seeds as a high-efficiency adsorbent for amoxicillin removal: kinetic, isotherm and thermodynamic studies. Chem Eng J. 2016;288:778–88. https://doi.org/10.1016/j.cej.2015.12.042.
60. Kragović M, Stojmenović M, Petrović J, Loredo J, Pašalić S, Nedeljković A, Ristović I. Influence of alginate encapsulation on point of zero charge (pHpzc) and thermodynamic properties of the natural and Fe(III)—modified zeolite. Procedia Manuf. 2019;32:286–93. https://doi.org/10.1016/j.promfg.2019.02.216.
61. Hassan AF, Abdel-Mohsen AM, Fouda MMG. Comparative study of calcium alginate, activated carbon, and their composite beads on methylene blue adsorption. Carbohydr Polym. 2014;102:192–8. https://doi.org/10.1016/j.carbpol.2013.10.104.
62. Cansado IPP, Belo CR, Mourão PAM. Pesticides abatement using activated carbon produced from a mixture of synthetic polymers by chemical activation with KOH and K_2CO_3. Environ Nanotechnol Monit Manag. 2019;12: 100261. https://doi.org/10.1016/j.enmm.2019.100261.
63. Nascimento RF, Lima ACA, Vidal CB, Melo DQ, Raulino GSCR Adsorção: aspectos teóricos e aplicações ambientais. Org. Ivanaldo Maciel de Lima. Fortaleza: Imprensa Universitária. 2014;256. http://www.repositorio.ufc.br/bitstream/riufc/10267/1/2014_liv_rfdnascimento.pdf. Accessed 15 May 2020.
64. Zhang X, Xu J, Lv Z, Wang Q, Ge H, Wang X, Hong B. Preparation and utilization of cigarette filters based activated carbon for removal CIP and SDS from aqueous solutions. Chem Phys Lett. 2020;747:137343. https://doi.org/10.1016/j.cplett.2020.137343.
65. Smidt E, Meissl K. The applicability of Fourier transform infrared (FT-IR) spectroscopy in waste management. Waste Manag. 2007;27:268–76. https://doi.org/10.1016/j.wasman.2006.01.016.
66. Wibawa PJ, Nur M, Asyari Nur H. SEM, XRD and FTIR analyses of both ultrasonic and heat generated activated carbon black microstructures. Heliyon. 2020;6(3):e03546. https://doi.org/10.1016/j.heliyon.2020.e03546.
67. Silverstein RM, Webster FX, Kiemle DJ, Bryce DL. Spectrometric identification of organic compounds. 8th ed. Hoboken: Wiley; 2014. p. 464.
68. Schulz H, Baranska M. Identification and quantification of valuable plant substances by IR and Raman spectroscopy. Vib Spectrosc. 2007;43:13–25. https://doi.org/10.1016/j.vibspec.2006.06.001.
69. Socrates G. Infrared and Raman characteristic group frequencies: tables and charts. 3rd ed. West Sussex: Wiley; 2001.
70. Nakamoto K. Infrared and Raman spectra of inorganic and coordination compounds part B: Applications in coordination, organometallic, and bioinorganic chemistry. 6th ed. Hoboken: Wiley; 2009. p. 2009.
71. de Costa PD, Furmanski LM, Dominguini L. Production, characterization and application of activated carbon from nutshell for adsorption of methylene blue. Revista Virtual de Química. 2015;7(4):1272–85. https://doi.org/10.5935/1984-6835.20150070.

72. Zhang Y, Song X, Xu Y, Shen H, Kong X, Xu H. Utilization of wheat bran for producing activated carbon with high specific surface area via NaOH activation using industrial furnace. J Clean Prod. 2019;10:366–75. https://doi.org/10.1016/j.jclepro.2018.11.041.
73. Liew RK, Azwar E, Yek PNY, Lim XY, Cheng CK, Ng J-H, Jusoh A, Lam WH, Ibrahim MD, Ma NL, Lam SS. Microwave pyrolysis with KOH/NaOH mixture activation: a new approach to produce micro-mesoporous activated carbon for textile dye adsorption. Bioresour Technol. 2018;266:1–10. https://doi.org/10.1016/j.biortech.2018.06.051.
74. Ibrahim WM, Hassan AF, Azab YA. Biosorption of toxic heavy metals from aqueous solution by *Ulva lactuca* activated carbon. Egypt J Basic Appl Sci. 2016;3(3):241–9. https://doi.org/10.1016/j.biortech.2018.06.051.
75. Archin S, Sharifi H, Asadpour G. Optimization optimization and modeling of simultaneous ultrasound-assisted adsorption of binary dyes using activated carbon from tobacco residues: response surface methodology. J Clean Prod. 2019;239:118136. https://doi.org/10.1016/j.jclepro.2019.118136.
76. IUPAC - International Union of Pure and Applied Chemistry. Reporting physisorption data for gas/solid systems with special reference to the determination of surface area and porosity. Pure Appl Chem. 1985;57:603–19.
77. Al-Ghouti MA, Da'ana DA. Guidelines for the use and interpretation of adsorption isotherm models: a review. J Hazard Mater. 2020;393:122383. https://doi.org/10.1016/j.jhazmat.2020.122383.
78. Kajama MN, Nwogu NC, Gobina E. Hydrogen permeation using nanostructured silica membranes. Sustain Dev Plan VII. 2015;193:447–56. https://doi.org/10.2495/SDP150381.
79. Ladavos AK, Ap K, Iosifidis A, Triantafyllidis KS, Pinnavaia TJ, Pomonis PJ. The BET equation, the inflection points of N_2 adsorption isotherms and the estimation of specific surface area of porous solids. Microporous Mesoporous Mater. 2012;151:126–33. https://doi.org/10.1016/j.micromeso.2011.11.005.
80. Gonçalves AC Jr, Schwantes D, Campagnolo MA, Dragunski DC, Tarley CRT, Silva AKS. Removal of toxic metals using endocarp of açaí berry as biosorbent. Water Sci Technol. 2018;77(6):1547–57. https://doi.org/10.2166/wst.2018.032.
81. Moussout H, Ahlafi H, Aazza M, Maghat H. Critical of linear and non-linear equations of pseudo-first order and pseudo-second order kinetic models. Karbala Int J Mod Sci. 2018;4(2):244–54. https://doi.org/10.1016/j.kijoms.2018.04.001.
82. Pholosi A, Naidoo EB, Ofomaja AE. Intraparticle diffusion of Cr(VI) through biomass and magnetite coated biomass: a comparative kinetic and diffusion study. S Afr J Chem Eng. 2020;32:39–55. https://doi.org/10.1016/j.sajce.2020.01.005.
83. Müller LC, Alves AAA, Mondardo RI, Sens ML. Methylene blue adsorption in *Pinus elliottii* (pine) and *Drepanostachyum falcatum* (bamboo) sawdust. Eng Sanit Ambient. 2019;24(4):687–95. https://doi.org/10.1590/S1413-41522019160344.
84. Tian Y, Li J, Whitcombe TW, McGill WB, Thring R. Application of oily sludge-derived char for lead and cadmium removal from aqueous solution. Chem Eng J. 2020;384:123386. https://doi.org/10.1016/j.cej.2019.123386.
85. Neta JJS, Silva CJ, Moreira GM, Reis C, Reis EL. Removal of the reactive blue 21 and direct red 80 dyes using seed residue of *Mabea fistulifera* Mart. as biosorbent. Rev Ambient Água. 2012;7(1):104–19. https://doi.org/10.4136/1980-993X.
86. Taiwo AF, Chinyere NJ. Sorption characteristics for multiple adsorption of heavy metal ions using activated carbon from Nigerian Bamboo. J Mater Sci Chem Eng. 2016;04:39–48. https://doi.org/10.4236/msce.2016.44005.
87. Barret EP, Joyner LG, Halenda PP. The determination of pore volume and area distributions in porous substances. Computation from nitrogen isotherms. J Am Chem Soc. 1951;73:373–80. https://doi.org/10.1021/ja01145a126.
88. Jeppu GP, Clement TP. A modified Langmuir–Freundlich isotherm model for simulating pH-dependent adsorption effects. J Contam Hydrol. 2012;129–130:46–53. https://doi.org/10.1016/j.jconhyd.2011.12.001.
89. Alyasi H, Mackey HR, Loganathan K, McKay G. Adsorbent minimisation in a two-stage batch adsorber for cadmium removal. J Ind Eng Chem. 2020;81:153–60. https://doi.org/10.1016/j.jiec.2019.09.003.
90. Vilela PB, Matias CA, Dalalibera A, Becegato VA, Paulino AT. Polyacrylic acid-based and chitosan-based hydrogels for adsorption of cadmium: equilibrium isotherm, kinetic and thermodynamic studies. J Environ Chem Eng. 2019;7(5):103327. https://doi.org/10.1016/j.jece.2019.103327.
91. Hu Q, Zhang Z. Application of Dubinin–Radushkevich isotherm model at the solid/solution interface: a theoretical analysis. J Mol Liq. 2019;277:646–8. https://doi.org/10.1016/j.molliq.2019.01.005.
92. Lima EC, Adebayo MA, Machado FM. Kinetic and equilibrium models of adsorption. In: Bergmann C, Machado F, editors. Carbon nanomaterials as adsorbents for environmental and biological applications. Cham: Springer; 2015. p. 33–69. https://doi.org/10.1007/978-3-319-18875-1_3.
93. Prola LDT, Machado FM, Bergmann CP, Souza FE, Gally CR, Lima EC, Adebayo MA, Dias SLP, Calvete T. Adsorption of direct blue 53 dye from SSE% first-order SSE% pseudo-second-order aqueous solutions by multi-walled carbon nanotubes and activated carbon. J Environ Manag. 2013;130:166–75. https://doi.org/10.1016/j.jenvman.2013.09.003.
94. Hajati S, Ghaedi M, Yaghoubi S. Local, cheep and nontoxic activated carbon as efficient adsorbent for the simultaneous removal of cadmium ions and malachite green: optimization by surface response methodology. J Ind Eng Chem. 2015;21:760–7. https://doi.org/10.1016/j.jiec.2014.04.009.
95. Shami RB, Shojaei V, Khoshdast H. Efficient cadmium removal from aqueous solutions using a sample coal waste activated by rhamnolipid biosurfactant. J Environ Manag. 2019;231:1182–92. https://doi.org/10.1016/j.jenvman.2018.03.126.
96. Sharma G, Naushad M. Adsorptive removal of noxious cadmium ions from aqueous medium using activated carbon/zirconium oxide composite: isotherm and kinetic modelling. J Mol Liq. 2020;310:113025. https://doi.org/10.1016/j.molliq.2020.113025.
97. Thabede PM, Shooto ND, Xaba T, Naidoo EB. Adsorption studies of toxic cadmium(II) and chromium(VI) ions from aqueous solution by activated black cumin (*Nigella sativa*) seeds. J Environ Chem Eng. 2020;8(4):104045. https://doi.org/10.1016/j.jece.2020.104045.
98. Zaheer Z, Al-Asfar A, Aazam ES. Adsorption of methyl red on biogenic Ag@Fe nanocomposite adsorbent: Isotherms, kinetics and mechanisms. J Mol Liq. 2019;283:287–98. https://doi.org/10.1016/j.molliq.2019.03.030.
99. Mishra AP, Ghosh MR. Use of silver impregnated activated carbon (SAC) for Cr(VI) removal. J Environ Chem Eng. 2020;8(1):103641. https://doi.org/10.1016/j.jece.2019.103641.
100. Alves SCS, Coseglio BB, Pinto LAA, Cadaval TRS Jr. Development of spirulina/chitosan foam adsorbent for phenol adsorption. J Mol Liq. 2020;309:113256. https://doi.org/10.1016/j.molliq.2020.113256.
101. Kajjumba WG, Emik S, Öngen A, Kurtulus ÖH, Aydin S. Modelling of adsorption kinetic processes —errors, theory and application. In: Edebali S, editor. Advanced sorption process applications. London: IntechOpen; 2018. p. 1–19. https://doi.org/10.5772/intechopen.80495.

102. Sahin R, Tapadia K. Comparison of linear and non-linear models for the adsorption of fluoride onto geo-material: limonite. Water Sci Technol. 2015;72(12):2262–9. https://doi.org/10.2166/wst.2015.449.
103. Markandeya SSP, Kisku GC. Linear and non-linear kinetic modeling for adsorption of disperse dye in batch process. Res J Environ Toxicol. 2015;9:320–31. https://doi.org/10.3923/rjet.2015.320.331.
104. Can M. Studies of the kinetics for rhodium adsorption onto gallic acid derived polymer: the application of non-linear regression analysis. System. 2015;127(4):1308–10. https://doi.org/10.12693/APhysPolA.127.1308.
105. Nagy B, Mânzatu C, Măicăneanu A, Indolean C, Barbu-Tudoran L, Majdik C. Linear and non-linear regression analysis for heavy metals removal using *Agaricus bisporus* macrofungus. Arabian J Chem. 2017;10:3569–79. https://doi.org/10.1016/j.arabjc.2014.03.004.
106. Qayoom A, Kazmi SA, Ali SN. Equilibrium modelling for adsorption of aqueous Cd(II) onto turmeric: linear versus non-linear regression analysis. Mor J Chem. 2017;5(2):362–70. https://revues.imist.ma/index.php?journal=morjchem&page=article&op=view&path%5B%5D=6548. Accessed 15 May 2020.
107. Piela L. Chapter 5—intermolecular interactions. In: Piela Lucjan, editor. Ideas of quantum chemistry. 3rd ed. Amsterdam: Elsevier; 2020. p. 337–436.
108. Stone AJ. Chapter 1—physical basis of intermolecular interactions. In: de la Roza AO, DiLabio GA, editors. Non-covalent interactions in quantum chemistry and physics. Amsterdam: Elsevier; 2017. p. 3–26. https://doi.org/10.1016/B978-0-12-809835-6.00002-5.
109. Coelho GF, Gonçalves AC Jr, Schwantes D, Álvarez-Rodríguez E, Tarley CRT, Dragunski D, Conradi E Jr. Removal of Cd(II), Pb(II) and Cr(III) from water using modified residues of *Anacardium occidentale* L. Appl Water Sci. 2018;8:96. https://doi.org/10.1007/s13201-018-0724-8.
110. Brasil. Conselho Nacional do Meio Ambiente (CONAMA). Resolução CONAMA n. 430, de 13 de maio de 2011. Brasília, DF. 2011;9. http://www2.mma.gov.br/port/conama/legiabre.cfm?codlegi=646. Accessed 15 Mar 2020.
111. Brasil. Ministério da Saúde. Portaria n° 2.914. Brasília, DF. 2011;33. http://bvsms.saude.gov.br/bvs/saudelegis/gm/2011/prt2914_12_12_2011.html. Accessed 15 Mar 2020.
112. Aljeboree AM, Alshirifi AN, Alkaim AF. Kinetics and equilibrium study for the adsorption of textile dyes on coconut shell activated carbon. Arab J Chem. 2017;10:S3381–93. https://doi.org/10.1016/j.arabjc.2014.01.020.
113. Kasperiski FM, Lima EC, Umpierres CS, Reis GS, Thue PS, Lima DR, Dias SLP, Saucier C, Costa JB. Production of porous activated carbons from *Caesalpinia ferrea* seed pod wastes: highly efficient removal of captopril from aqueous solutions. J Clean Prod. 2018;197:919–29. https://doi.org/10.1016/j.jclepro.2018.06.146.